NASA TECHNICAL NOTE

NASA TN D-7911

NASA TN D-7911

A MULTISENSOR ANALYSIS OF NIMBUS-5 DATA RECORDED ON JANUARY 22, 1973

L. J. Allison, E. B. Rodgers, T. T. Wilheit, and R. Wexler

Goddard Space Flight Center
Greenbelt, Md. 20771

NATIONAL AERONAUTICS AND SPACE ADMINISTRATION • WASHINGTON, D. C. • MARCH 1975

1. Report No.	2. Government Accession No.	3. Recipient's Catalog No.
NASA TN D-7911		

4. Title and Subtitle	5. Report Date
A Multisensor Analysis of Nimbus-5 Data Recorded on January 22, 1973	6. Performing Organization Code: 910
7. Author(s) L. J. Allison, E. B. Rodgers, T. T. Wilheit, and R. Wexler	8. Performing Organization Report No.: G-7507
9. Performing Organization Name and Address: Goddard Space Flight Center, Greenbelt, Maryland 20771	10. Work Unit No.: 175-61-41-01
	11. Contract or Grant No.
	13. Type of Report and Period Covered: Technical Note
12. Sponsoring Agency Name and Address: National Aeronautics and Space Administration, Washington, D. C. 20546	14. Sponsoring Agency Code

15. Supplementary Notes

16. Abstract

The Nimbus-5 meteorological satellite has a full complement of radiation sensors. Data from these sensors obtained on January 22, 1973, were analyzed and intercompared for orbits 569 and 570. The electrically-scanning microwave radiometer (19.35-GHz region) delineated rain areas over the ocean off the U. S. east coast, in good agreement with WSR-57 and FPS-77 radar imagery, and permitted the estimation of rainfall rates in this region. Residual ground water, from abnormal rainfall in the lower Mississippi Valley, was indicated under clear sky conditions by soil brightness temperature values in the Nimbus-5 ESMR and U.S. Air Force Data Acquisition and Processing Program (DAPP) infrared data. The temperature-humidity infrared radiometer (6.7 μm and 11 μm) showed the height and spatial configuration of frontal clouds along the east coast and outlined the confluence of a polar jet stream with a broad subtropical jet stream along the U.S. Gulf Coast. Temperature profiles from three vertical temperature sounders were found to be in good agreement with related radiosonde ascents along orbit 569 from the subtropics to the Arctic Circle.

17. Key Words (Selected by Author(s))	18. Distribution Statement
Nimbus-5 microwave and infrared data, Rainfall rates, Radar images, Satellite images, Hydrology, Space sciences, Vertical sounders, Jet streams	Unclassified–Unlimited CAT.47

19. Security Classif. (of this report)	20. Security Classif. (of this page)	21. No. of Pages	22. Price*
Unclassified	Unclassified	43	$3.75

* For sale by the National Technical Information Service, Springfield, Virginia 22151.

This document makes use of international metric units according to the Systeme International d'Unites (SI). In certain cases, utility requires the retention of other systems of units in addition to the SI units. The conventional units stated in parentheses following the computed SI equivalents are the basis of the measurements and calculations reported.

CONTENTS

A MULTISENSOR ANALYSIS OF NIMBUS-5 DATA RECORDED ON JANUARY 22, 1973

L. J. Allison
Goddard Space Flight Center

E. B. Rodgers
Environmental Research and Technology, Inc.

T. T. Wilheit and R. Wexler
Goddard Space Flight Center

INTRODUCTION

Nimbus-5, launched on December 11, 1972, is a research and development satellite equipped with the electrically-scanning microwave radiometer (ESMR), a promising new tool for global synoptic weather analysis. This instrument recorded microwave radiometric measurements through clouds, and inferred new meteorological and hydrological parameters not detectable by previous visible or infrared satellite sensors (Skidmore and Purdom, 1973).

The purpose of this paper is to describe the ESMR experiment and make multisensor data comparisons with the temperature-humidity infrared radiometer (THIR), the infrared temperature profile radiometer (ITPR), the Nimbus-E microwave spectrometer (NEMS), the selective chopper radiometer (SCR), and meteorological radar and radiosonde data close to satellite-overpass time over the eastern United States, and to interpret the meteorological usefulness of the data for orbits 569 and 570 on January 22, 1973.

ELECTRICALLY-SCANNING MICROWAVE RADIOMETER EXPERIMENT

The electrically-scanning microwave radiometer (ESMR) was designed to measure earth and atmospheric radiation in the 19.35-GHz (1.55-cm) region from a polar orbit at approximately 1100-km altitude. The purposes in flying this experiment were to record and map passive microwave radiation patterns (in brightness temperature, T_B) for the delineation of areas of precipitation, to derive cloud liquid-water content over the oceans, and to differentiate between cirrus and other ice crystal clouds and thick water-droplet clouds by comparison with simultaneous observations in the visible and infrared channels.

Other aims of this research program were to observe and demarcate areas of sea ice and open sea in the polar regions regardless of cloud cover, and to test the feasibility of inferring soil moisture providing that no heavy clouds exist over the area of interest.

The feasibility of the basic microwave measurements over the oceans, land, and sea ice, prior to the Nimbus-5 launch had been established by NASA Convair 990 flights with the aircraft prototype model of ESMR, which also provided check-of-calibration ground-truth observations under the satellite after launch. (See Catoe et al., 1967; Nordberg et al., 1969; Gloersen et al., 1972, 1973 (a), (b), and (c); Schmugge et al., 1972; and Wilheit el al., 1972.)

The application of passive microwave techniques to the ocean surface has been documented by Paris, 1969, 1971; Hollinger, 1971; Ross et al., 1970; and Nordberg et al., 1971. These studies related the microwave signature of the ocean and atmosphere to sea state, surface temperature, salinity, and atmospheric moisture (U. S. Department of Commerce, 1971).

Martin and Scherer (1973), in their review of present satellite rainfall estimate methods, discuss the value of making rainfall estimates globally. They note that precipitation is a sensitive indicator of the amount and distribution of the release of latent heat of condensation, the upward mass flux, and the spatial organization of convection. The accurate estimate of precipitation is important in studies of the heat and water budget over convective clouds, with special emphasis during the Data Systems Test and GATE in 1974 ("GARP Project Data Systems Test Plan," GSFC, 1973). Since previous satellite sensor systems cannot directly detect rain in its liquid or near-frozen state (Follansbee, 1973), the ESMR data were needed to fill the gap in this vital, global observational study.

FUNDAMENTAL PHYSICAL RELATIONSHIPS

In the microwave region, Planck's formula for the spectral intensity of thermal radiation emitted by a surface is given by the Rayleigh-Jeans approximation (Leighton, 1959):

$$I(\lambda,T) = \frac{e2\pi c k T}{\lambda^4}$$

where:

- T = thermodynamic temperature,
- k = Boltzmann's constant,
- λ = wavelength,
- c = velocity of light,
- e = emissivity of surface,
- I = emission per unit area per unit wavelength interval,
- T_B = brightness temperature.

I is directly proportional to the temperature (T), hence the thermal radiation is approximately proportional to the product of the emissivity and the actual temperature,

$$eT = \frac{I_\lambda \lambda^4}{2 \pi c k}$$

where:

$$T_B = eT.$$

The ESMR can measure brightness temperatures over the 180 K range, extending from 120 K to 300 K. Because the ocean has a low surface emissivity of 0.4 at 19.35 GHz, as compared with 0.85 to 0.95 and greater for nonvegetating ground surface, the T_B values under clear sky conditions are expected to range from 120 K to 160 K, depending on latitudinal variation of water content. Microwave radiation can penetrate nonraining clouds, although there is some minor attenuation. Large droplets in clouds and rain in the atmosphere below the freezing altitude, generally <4.5 km, have an enhanced absorption effect, due to an effective size dimension comparable to wavelength divided by the large index of refraction of water at microwave frequencies, and such droplets and rain are delineated by T_B values of 160 to 260 K over an ocean background (Gunn and East, 1954; Aerojet Electrosystems Co., 1973; and T.T. Wilheit, "The ESMR Experiment," *Nimbus-5 Users Guide,* NASA-GSFC, 1972).

Because the imaginary part of the dielectric constant of ice is so small at microwave frequencies, the absorption coefficient of ice crystals within cirrus cloud formations is negligible. At the ESMR frequency, there is no sensitivity to ocean salinity, but there is some effect at the nadir due to ocean roughness, streaks, and white cap cover (Nordberg, et al., 1971; Porter and Wentz, 1972).

THE ESMR INSTRUMENT AND SELECTED DATA EXAMPLES

The ESMR consists of a microwave receiver, which operates in the Dicke mode to eliminate low-frequency noise, plus associated electronics and an electrically-scanned planar array antenna, which is capable of receiving one polarization. The 90- by 90-cm radiometer antenna (figure 1), deployed after launch, scans the earth every 4 seconds, and views 50° on either side of nadir in 78 steps with some overlap. The radiometric scanning process is controlled by an onboard computer; this permits the recording of brightness temperature within a noise equivalent temperature change (NEΔT) of approximately 2 K, from a 25-km scan spot at nadir, to a 45- by 165-km scan spot at 50° nadir angle (T.T. Wilheit, "The ESMR Experiment," *Nimbus-5 Users Guide,* NASA-GSFC, 1972). A cold reference temperature is obtained by using a sky horn which looks out at the cold radiant temperature of space. This space temperature was noted to be approximately 3 K in the 19.35-GHz frequency range. By monitoring two reference loads in the radiometer and the cold horn reference temperature, the observed radiometric temperature can be corrected to obtain system absolute brightness temperatures within ±1 K. The microwave radiation detected at the spacecraft is formatted on board by the versatile information processor (VIP), and stored with the atmospheric and other sensor data on the VIP track of the high data rate storage system (HDRSS) tape recorder. Data are telemetered to the ground at Fairbanks, Alaska, and Rosman, North Carolina, and are transmitted to GSFC for research studies.

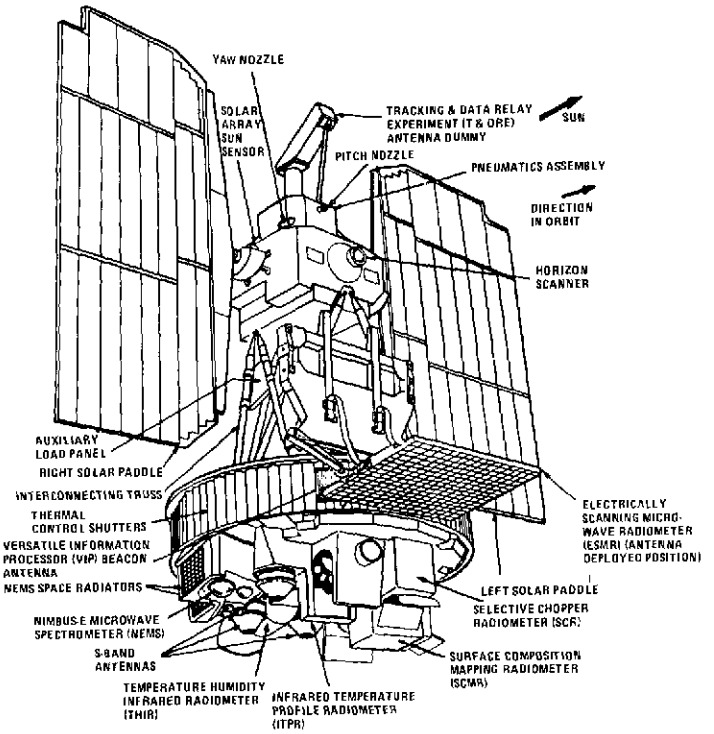

Figure 1. The Nimbus-5 spacecraft with associated experiments.

The following figures contain several examples of Nimbus-5 ESMR data, obtained from quick-look photofacsimile processing. Figure 2 shows three global montages from individual orbits 735 through 747 recorded on February 4, 1973. Three dynamic ranges are shown: montage 1 (138 to 210 K), montage 2 (194 to 256 K), and montage 3 (254 to 290 K).

By dividing the total brightness temperature range of ESMR data into three overlapping subranges, various meteorological and hydrological features are easily delineated. Montage 1 shows rainfall areas and variations in atmospheric moisture but no information is discernible over the dark land areas. Montage 2 indicates areas of intense rainfall over the oceans and shows contrasts between first year ice formations (dark) and older ice and snow (light). Montage 3 shows areas of heavy rainfall over oceans, high soil moisture, and snow cover over land areas. (For further details on more recent Nimbus-5 ESMR sea ice detection results, see Gloersen, et al., 1973, a, b, and c; Wilheit, et al., 1972; and Campbell, et al., 1973.)

Three examples of midlatitudinal frontal rain over the Pacific and Atlantic Oceans during December 1972 are shown in figure 3. Note the more diffuse rain areas shown in the warm front (a), the narrow dark line of rain within the prefrontal squall line in (b), and the occluded front (c). (A more comprehensive discussion of other synoptic cases using ESMR imagery may be found in studies by Wilheit, et al., 1973; Theon, 1973; and Sabatini and Merritt, 1973.)

Figure 2. Nimbus-5 ESMR photofacsimile global montages for February 4, 1973, daytime data orbits 735 through 747, 19.35 GHz.

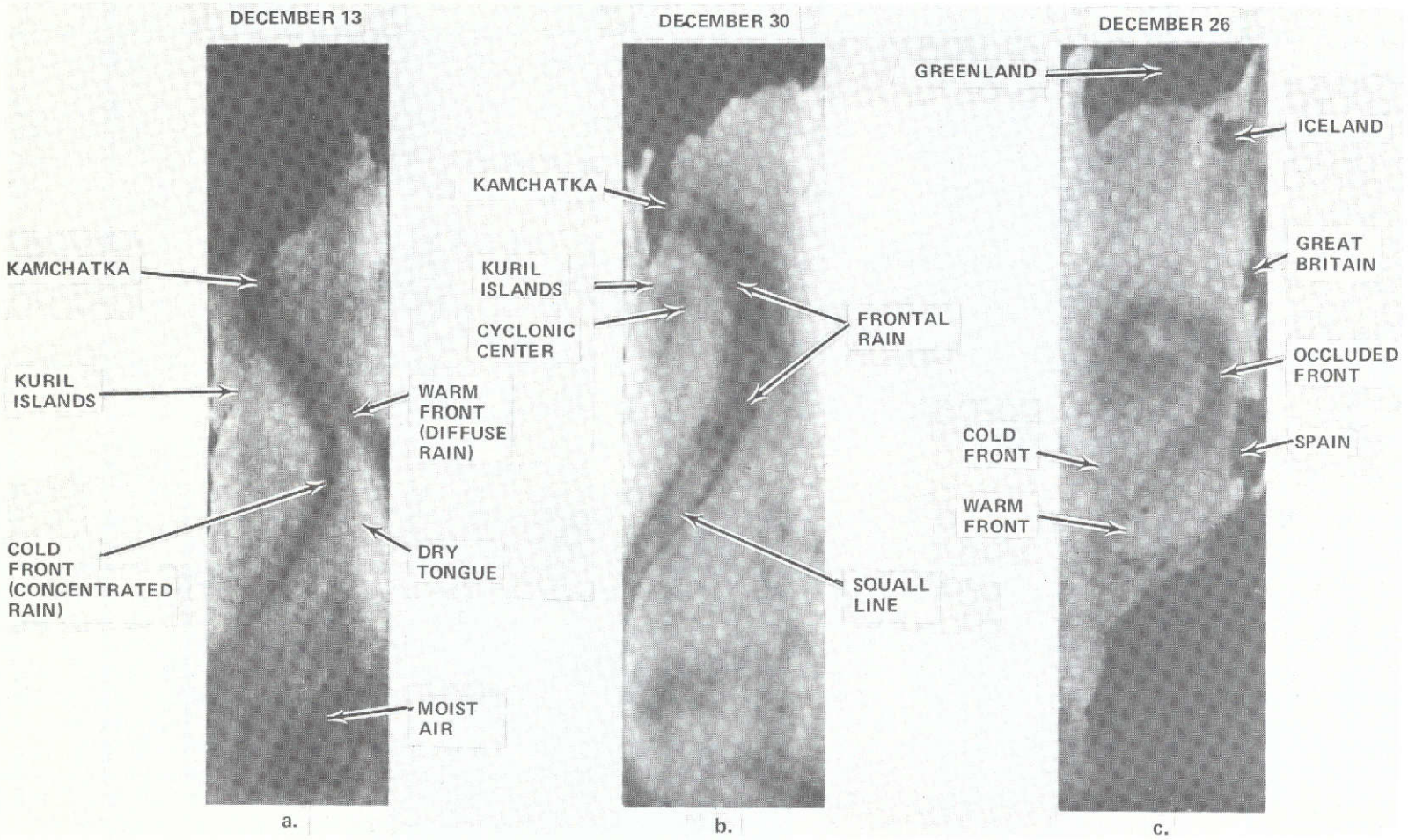

Figure 3. Nimbus-5 ESMR photofacsimile images of mid-latitude frontal systems during December 1972 (T_B range: 194 to 256 K) 19.35 GHz.

In order to verify ESMR data for exact locations of rain clouds in a frontal system over water off the U.S. east coast, simultaneous ground weather radar data were collected, coinciding with the Nimbus-5 over-flight during orbit 569 on January 22, 1973. With these meteorological data, correlative analysis was performed.

METEOROLOGICAL ANALYSIS OF JANUARY 22, 1973

In order to perform a thorough meteorological analysis of January 22, 1973, various types of ground weather data records and other satellite data were obtained for verification of the Nimbus-5 data of orbit 569. The 1800 GMT National Meteorological Center (NMC) surface weather chart (figure 4) shows the location of an active cold front, oriented NE/SW off the east coast of the U.S. which was moving southeastward through central Florida. Cloud remnants of the associated decaying occlusion, which was located over the Midwest and

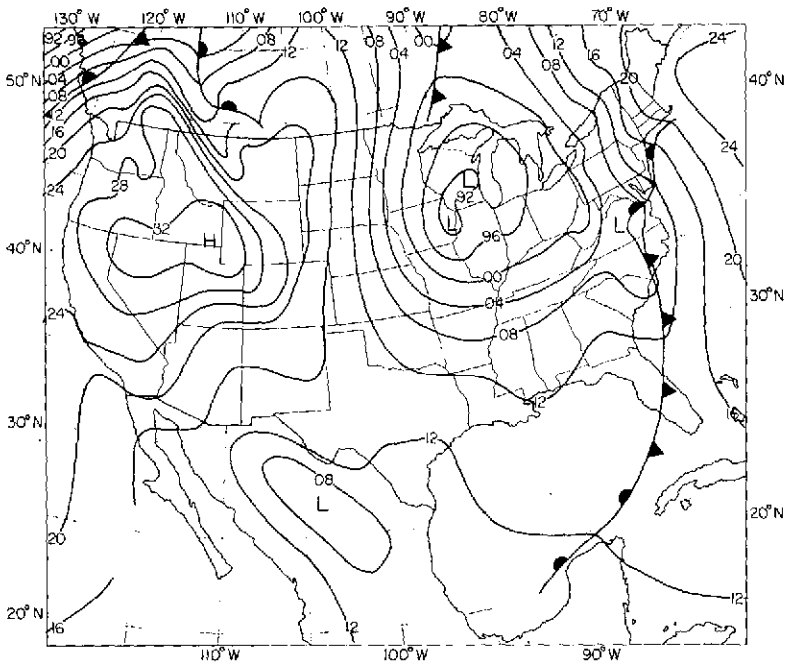

Figure 4. National Meteorological Center, National Weather Service North American surface chart, 1800 GMT, January 22, 1973 (24 line = 1024 millibars. Add 1,000 to numbers shown.)

Great Lakes region, were also recorded between 1600 and 1800 GMT by the U.S. Air Force Data Acquisition and Processing Program (DAPP)* and the ATS-3 and Nimbus-5 (THIR) satellites (figures 5a, 5b, and 5c, respectively).

*DAPP is now known as Defense Meteorological Satellite Program (DMSP).

Figure 5a. U. S. Air Force Data Acquisition and Processing Program (DAPP) image of visual data (0.4 to 1.1 μm, day), 1600-1800 GMT, January 22, 1973, 617.3 m (1/3 n.m.) resolution.

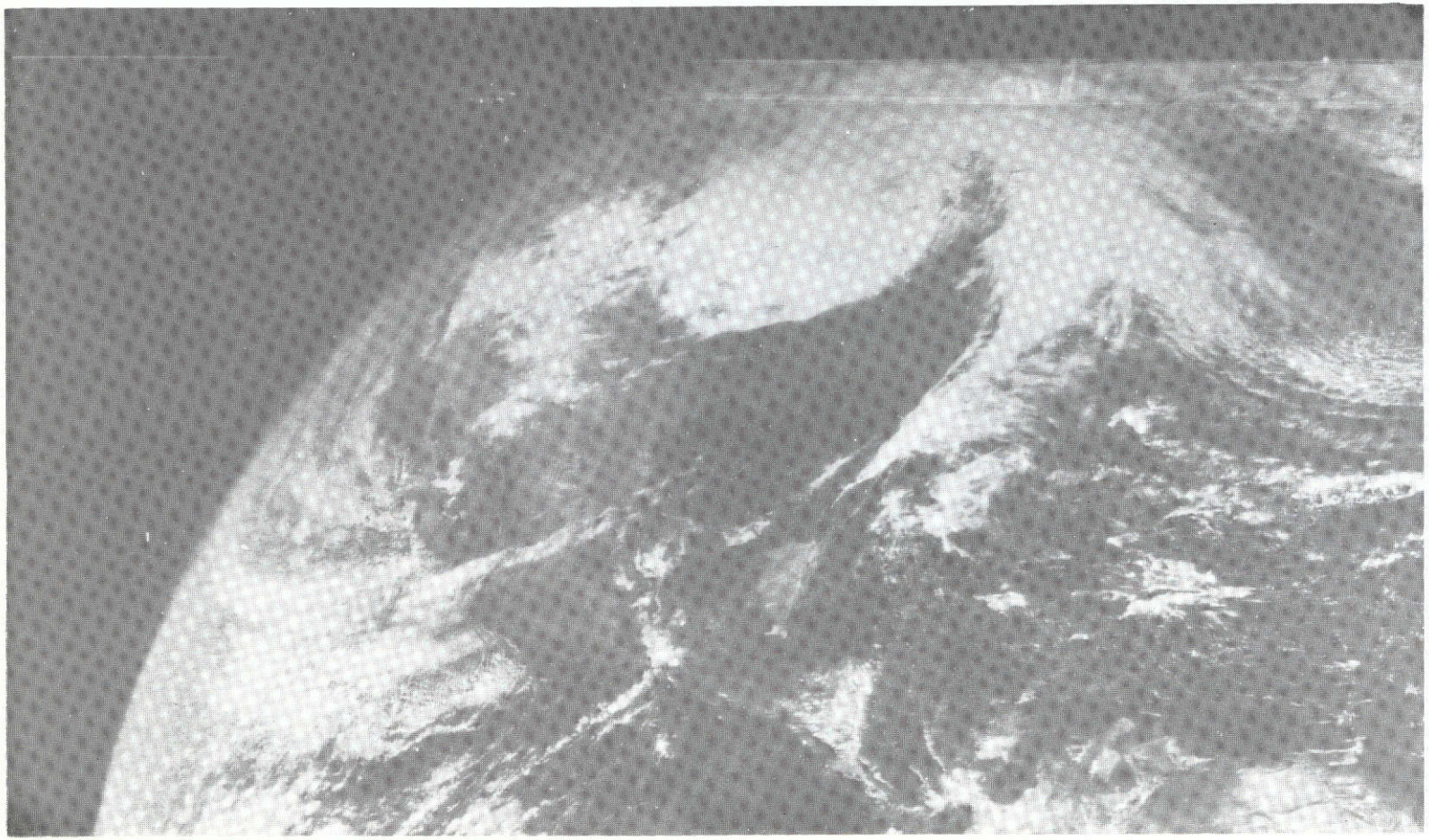

Figure 5b. ATS-3 image recorded at 1704 GMT, January 22, 1973.

Figure 5c. Nimbus-5 THIR photofacsimile image daytime orbit 569, January 22, 1973 (11 μm).

A Nimbus-5 ESMR photofacsimile picture of orbit 569 and the associated 1:5 million Mercator digital grid print map are shown in figures 6a and 6b respectively. Note that the Great Lakes appear quite cold (150 to 180 K, white tone) even through overcast clouds, and the heavy frontal rain off the Florida coast appears dark gray (160 to >240 K). The National Weather Service radar summary for 1640 GMT, January 22, 1973 (figure 7) shows 25,000 to 41,000-foot (7,600 to 12,500 m) tops over a line of thunderstorms through central Florida, while lower heights of 20,000 to 22,000 feet (6,000 to 6,700 m) were recorded over lighter rain showers further to the north. Scattered rain and snow showers are shown in figure 7 to the west over the north-central Mississippi Valley and Great Lakes region. These showers are within the slowly-filling occlusion which appears as light gray in figure 6a (left).

Figure 6a. Nimbus-5 ESMR photofacsimile image, orbit 569, January 22, 1973, 19.35 GHz.

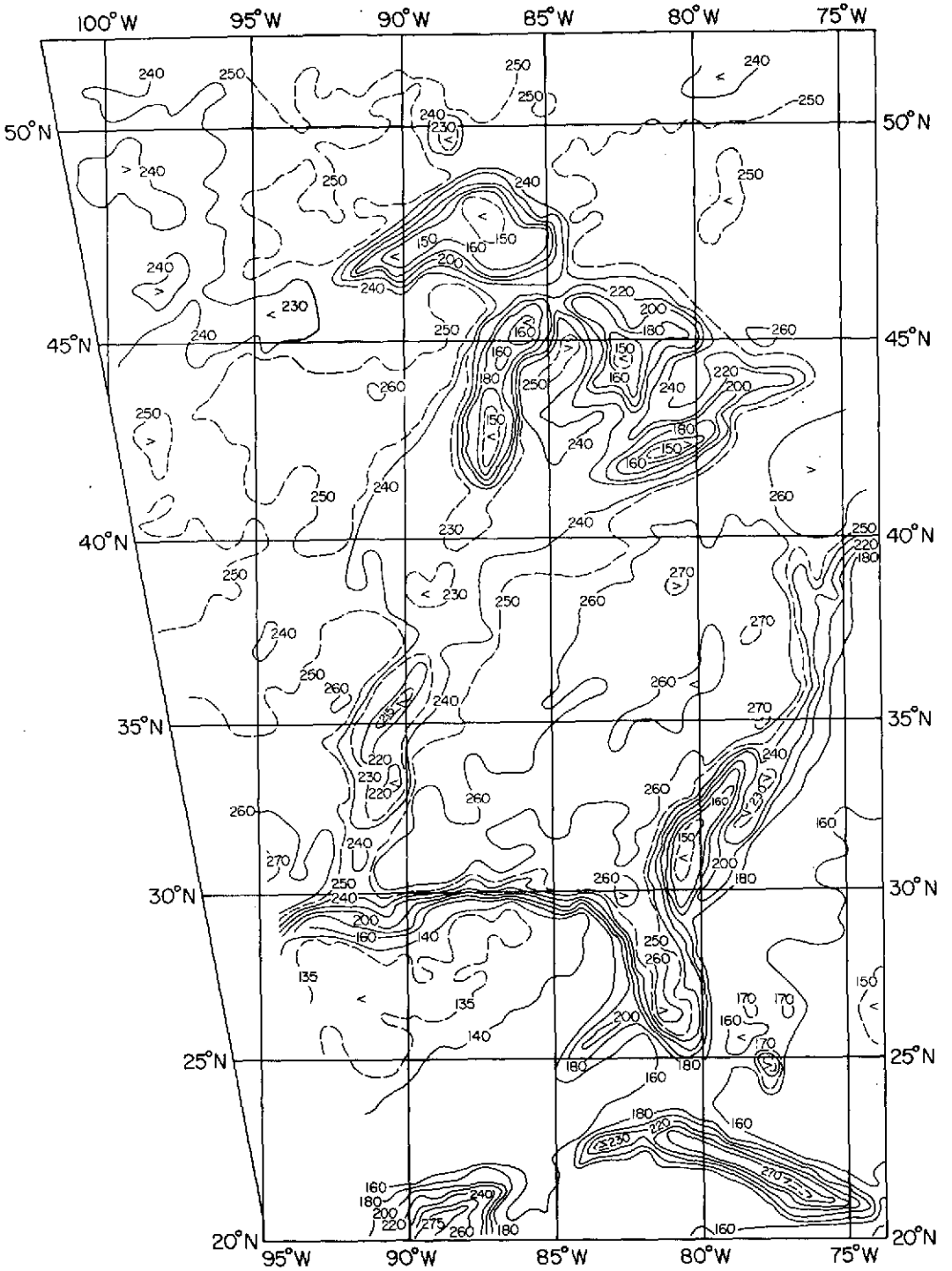

Figure 6b. Nimbus-5 ESMR grid print map analysis, 1:5 million Mercator, 1637 to 1648 GMT, orbit 569, January 22, 1973, 19.35 GHz, T_B in Kelvin.

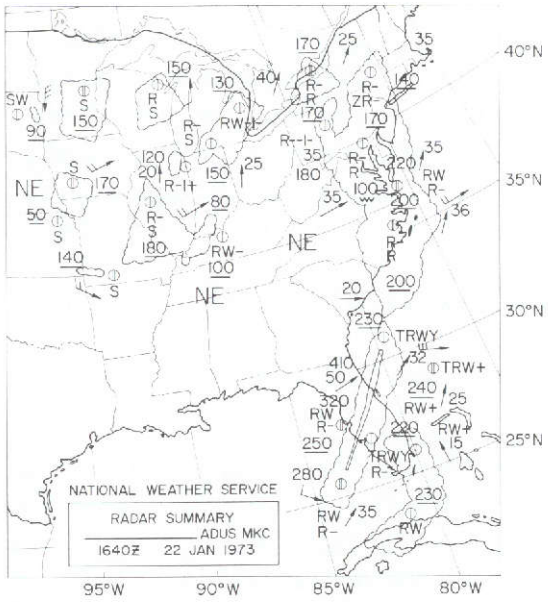

Figure 7. National Weather Service Radar Summary, 1640 GMT, January 22, 1973. Cloud tops in hundreds of feet.

A comprehensive effort was made to obtain all available Weather Service Radar (WSR-57) weather radar polaroid pictures taken within 10 minutes of Nimbus-5 satellite passage over the east coast. An example of data recorded at Daytona Beach is shown in figure 8a.

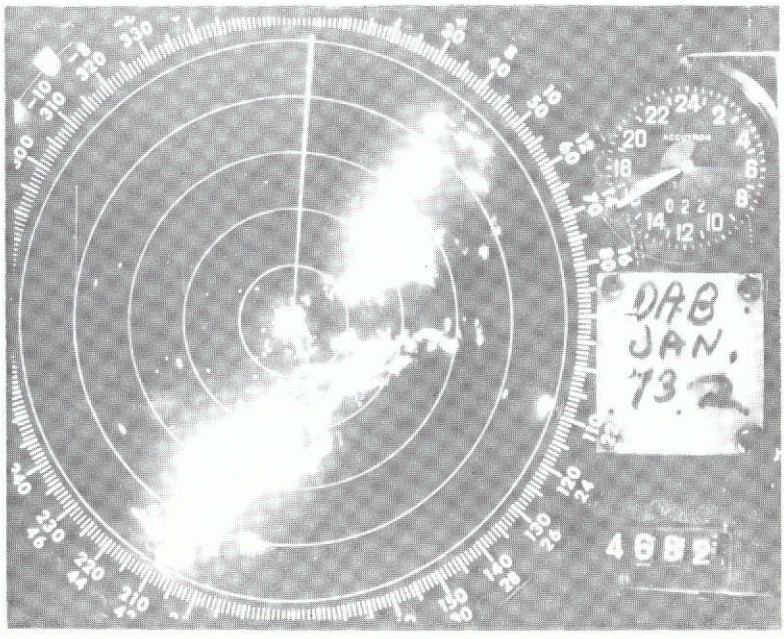

Figure 8a. National Weather Service WSR-57 (10 cm) weather radar PPI polaroid image, recorded 1640 GMT, January 22, 1973, at Daytona Beach, Florida, 40-km (25-mile) range markers.

The radar images were carefully relocated on a 1:2.5 million Mercator map, figure 8b. Note the overlap of radar echoes (darker hatching) between Wilmington-Hatteras, North Carolina, and Daytona Beach-Tampa, Florida. A large radar gap appears between 30° to 32°N just east of the Waycross, Georgia, radar site. However, the location of warm ESMR brightness temperatures T_B = 180 to > 220 K in the frontal zone (figure 8c) shows the rain to be continuous in that region. There is a good relationship between the ESMR brightness data (> 170 K) and radar rainfall echoes over the water southwest of Wilmington, North Carolina, and Tampa, Florida. Lake Okeechobee, located at approximately 27°N, 81°W, in south-central Florida, T_B of 230 to 240 K, and the west Florida coastline, T_B of 200 to 220 K, were used to more accurately position the ESMR data, which was in error by 1° latitude-longitude.

Figure 8d shows a 1:2.5 million Mercator digital grid print map of Nimbus-5 THIR (11-μm) data over the same area. A high cloud cluster, as indicated by T_B values < 230 K in the 11-μm imagery over the area of the radar gap off the Georgia coast implies the presence of rainshowers in that area. The high cloudiness at point A is a result of cirrus blowoff from thunderstorms in the vicinity of the subtropical jet stream. Note that these ice crystal clouds are not indicated by the ESMR data in figure 8c.

The other areas of cold T_B values in figure 8d (<230 K, indicated by dots) generally overlay rain echoes in figure 8b, and warmer ESMR T_B values in figure 8c (> 170 K). There is a good generalized inverse relationship between the ESMR brightness temperatures of frontal rain clouds over water and the 11-μm data. This pertains similarly to the post-frontal clearer-sky subsidence area off the South Carolina coast (30° to 32°N) and eastern Gulf of Mexico.

As a result of close coordination with the Air Weather Service at Cape Kennedy, Florida, FPS-77 radar data were recorded at 1641 GMT within two minutes of Nimbus-5, the overflight (orbit 569) in that area (figure 9a). Four levels of rainfall rate, in shades of gray, were obtained by using Plan Position Indication (PPI) polaroid pictures with the following criteria: 30 dB, 0.3 inch per hour; 35 dB, 0.5 inch per hour; 40 dB, 1 inch per hour; and 45 dB, 2 inches per hour. Note on figure 9a the small area of 0.3 inch per hour radar echoes in the 1° square in the top right-hand corner, and the large area of ESMR T_B values 200 to 220 K in figure 9b. At a range of 75 to 100 miles (120 to 160 km), with a 0.5° elevation angle, the FPS-77 radar can detect precipitation only at the 10,000 to 12,000-foot level, due to the earth's curvature. This height was the approximate freezing level for the area of the radar gap.

It is evident that the ESMR data provide more qualitative rainfall information than the ground weather radar, which has its physical limitations due to slant range, elevation angle, cloud dropsize distribution, and other attenuation factors (Battan, 1959). The 0.5 to 1 inch per hour isolines over water, east of Cape Kennedy, in figure 9a, overlay the 170- to 200-K brightness values in figure 9b. The 1 to 2 inches per hour rainfall isolines extending over land southwestward from Cape Kennedy in figure 9a are not clearly indicated in the ESMR

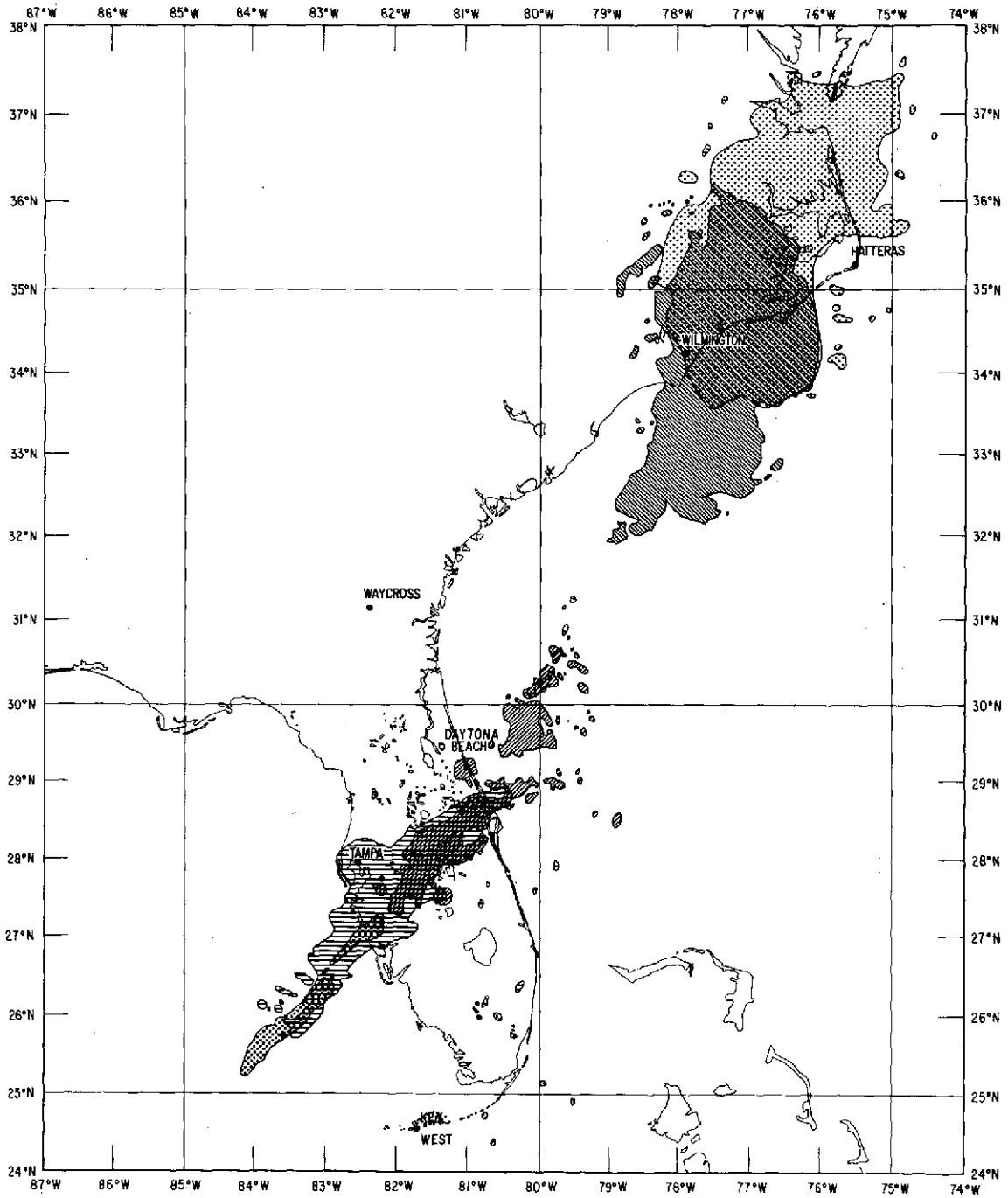

Figure 8b. Hand-rectified National Weather Service WSR-57 weather radar images from Key West, Tampa, and Daytona Beach, Florida, Waycross, Georgia, and Wilmington, and Hatteras, North Carolina, from 1637 to 1643 GMT, January 22, 1973. (Darker gray hatching indicates overlapping radar echoes.).

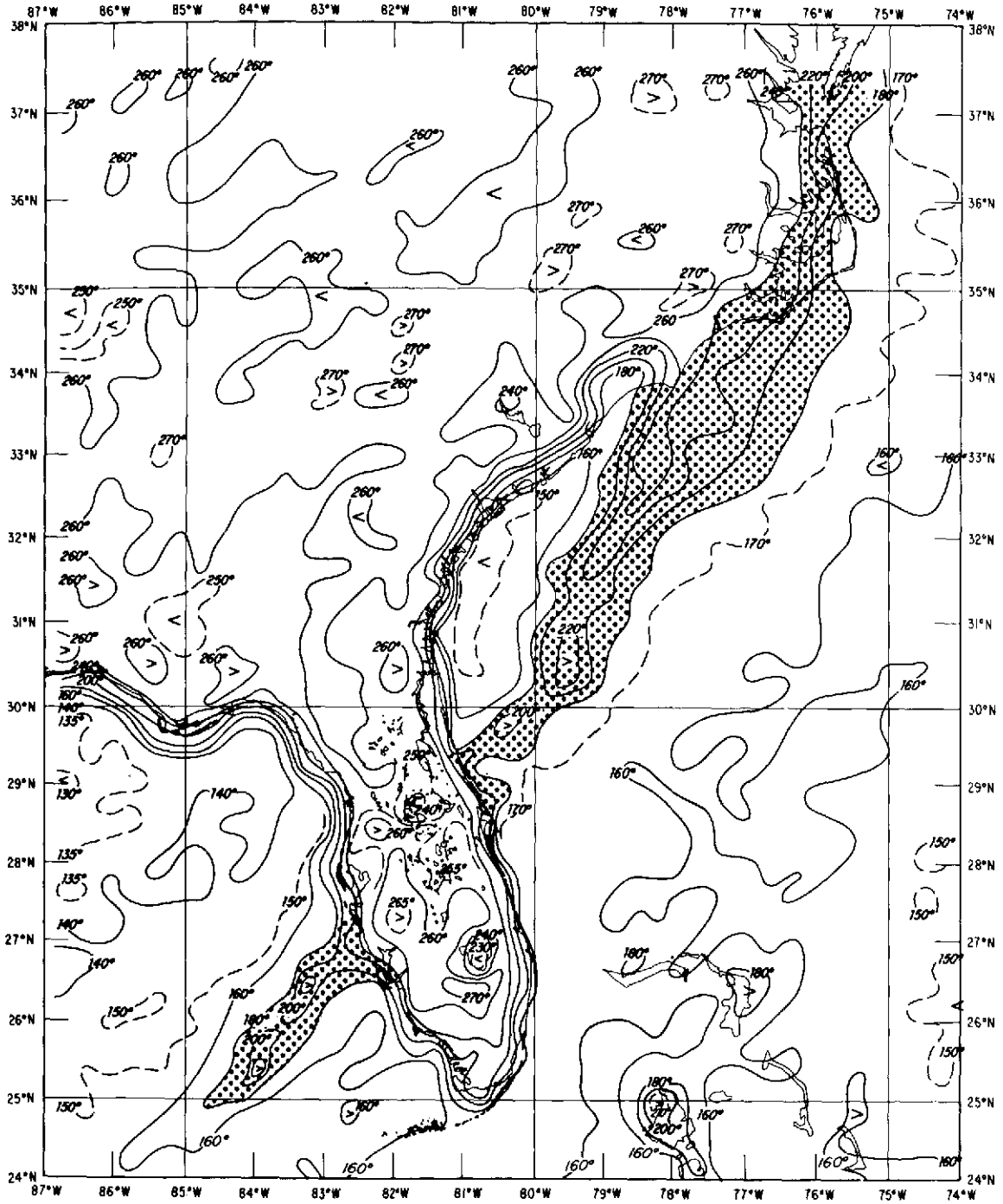

Figure 8c. Nimbus-5 ESMR grid print map analysis. T_B in K, 1:2.5 million Mercator, 1639 to 1643 GMT, orbit 569, January 22, 1973, 19.35 GHz. (Dotted area: T_B>180 K over water.)

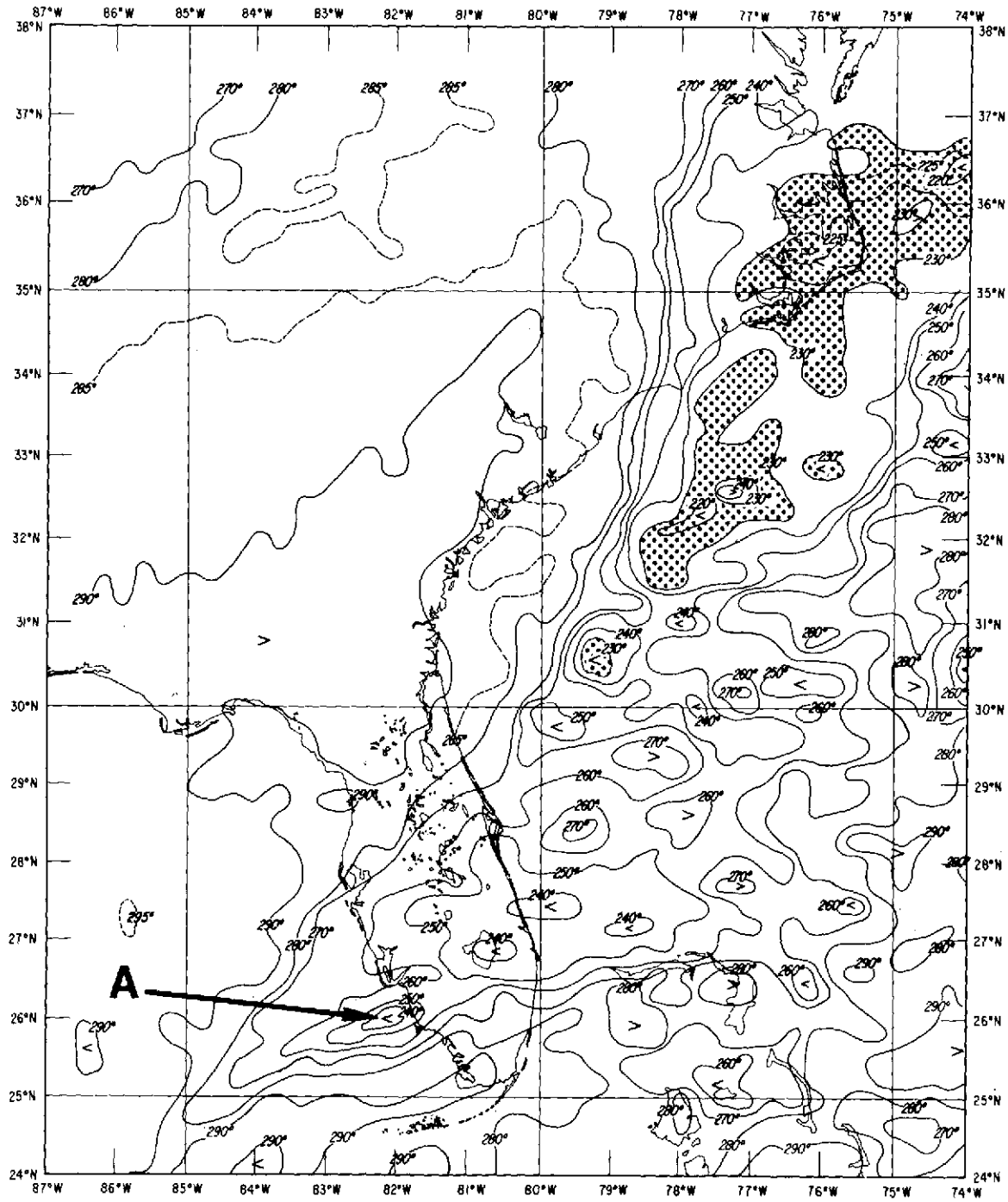

Figure 8d. Nimbus-5 THIR grid print map analysis, T_B in K, 1:2.5 million Mercator, 1639 to 1643 GMT, orbit 569, January 22, 1973, 11 μm. (Dotted area: T_B <230 K.) Arrow (A) indicates cirrus cloud blow-off in vicinity of subtropical jet stream.

brightness temperatures patterns in figure 9b. This may be due to the failure of the thin line of frontal thunderstorms to fill the whole field of view and/or mislocation of the ESMR scan spots by the computer program.

The effect of the complicated patterns of background radiance of the small lakes, swampland, forests, cultivated soils, and vegetation in central Florida must be measured daily under clear sky conditions by ESMR in order to understand the changes in ESMR brightness values during rainy periods. This makes the determination of actual rainfall rates over land extremely difficult.

A more detailed empirical study of nearly simultaneous ESMR and weather radar data over water was made using rainfall rates obtained from the VIP system on the WSR-57 radar set at Miami, Florida. In this analysis, data samplings of the ESMR brightness values were obtained from the Nimbus-5 brightness temperature tape, which gives time, latitude and longitude, and T_B values for all 50 scan positions from a limit of 30° left to 30° right of nadir, perpendicular to the spacecraft foreward velocity vector. The instantaneous field-of-view at the scan position near nadir is 25 by 25 km, degrading to approximately 30 by 40 km at 30° off nadir.

The VIP processes the radar's logarithmic receiver output to show six levels of rainfall intensity up to a 231-km (125-n.m.) range. The six intensity levels are contoured on the radar PPI scope for all echoes by use of a gray-scale. Rainfall hourly rates less than 2.5 mm, 2.5 to 12.7 mm, and 12.7 to 25.4 mm (less than 0.1 inch, 0.1 to 0.5 inch, and 0.5 to 1 inch) are shaded gray, white, and black, respectively. For rainfall rates of 25.4 to 50.8 mm, 50.8 to 127 mm, and greater than 127 mm (1 to 2 inches, 2 to 5 inches, and more than 5 inches) the shades are repeated, gray, white, and black.

Figures 10a and 10b show examples of the Nimbus-5 ESMR imagery and VIP, as displayed on the Miami PPI scope on February 15, 1973. An area of heavy rain is shown east of Miami on figure 10b, with rainfall rates between 50.8 and 127 mm per hour. On figure 10b each range circle on the scope represents 40 km (25 miles), and the rain cells recorded occurred within three minutes of the Nimbus-5 overflight.

In order to correlate rainfall rate versus ESMR T_B values, the T_B data were plotted by hand on a 1:3.168 million Mercator map of the Florida region. Because of a gridding error of approximately 1° latitude along the suborbital forward vector of the spacecraft, caused by the distortion of the antenna due to solar heating, the T_B analysis had to be fitted to the Florida coastline and Lake Okeechobee, using the warm T_B coastline gradient as a guide. The VIP radar image display was then superimposed on the T_B analysis and a point-by-point comparison was made. Because the instantaneous field-of-view for each beam position varied with different nadir angles, and sometimes resolved more than one rainfall intensity, the different rainfall intensity elements that fell within the instantaneous field-of-view were weighted in accordance to areal extent. Only rain elements that fell within a range of 40,000 to 200,000 meters (25 to 125 miles) over the ocean were considered.

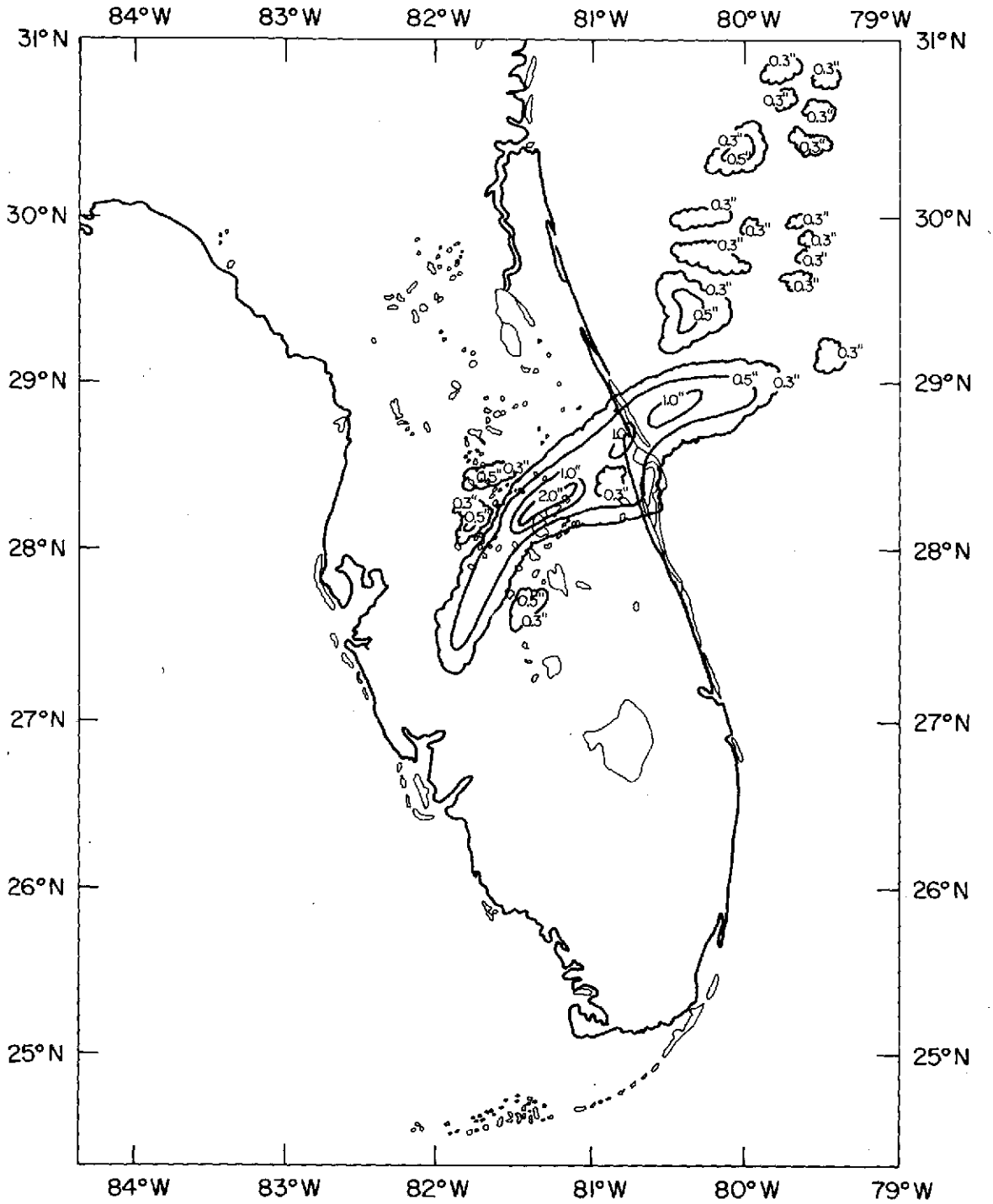

Figure 9a. U.S. Air Force, AWS FPS-77 (5.4 CM), Cape Kennedy, Florida, weather radar analyses, hand-rectified to 1:2.5 million Mercator map, 1641 GMT, January 22, 1973. Rainfall rate isolines are 0.3, 0.5, 1, and 2 inches (7.6, 12.7, 25.4, and 50.8 mm) per hour.

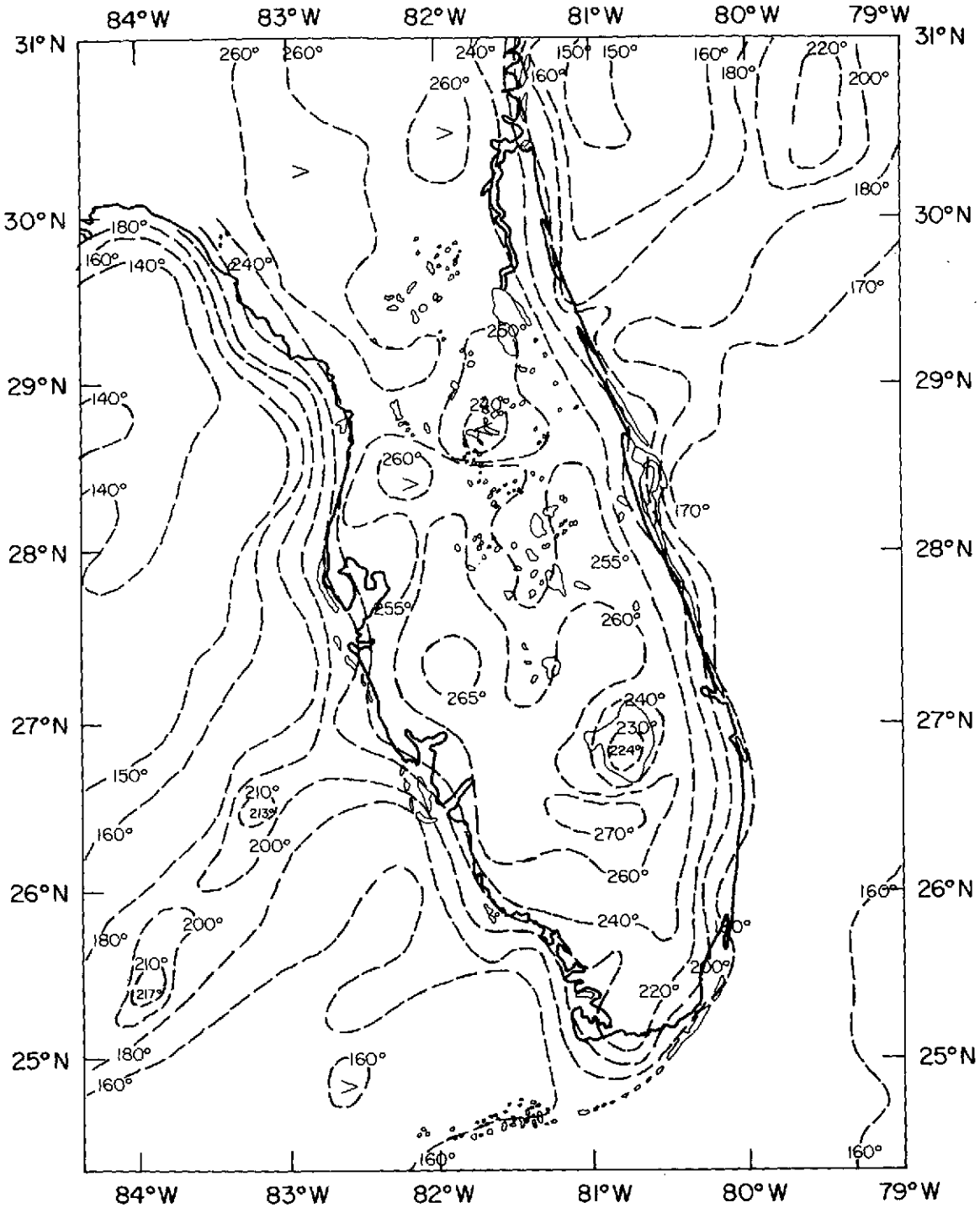

Figure 9b. Nimbus-5 ESMR grid print map analysis, T_B in K, 1:2.5 million Mercator, 1638 to 1641 GMT, orbit 569, January 22, 1973, 19.35 GHz.

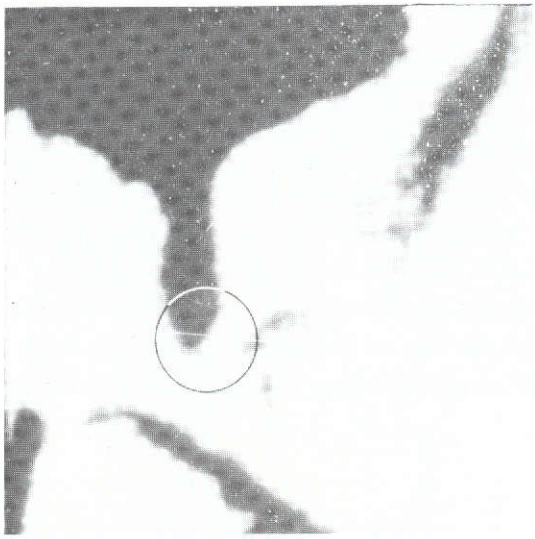

Figure 10a. Nimbus-5 ESMR photofacsimile image, orbit 891, 1623 GMT, February 15, 1973.

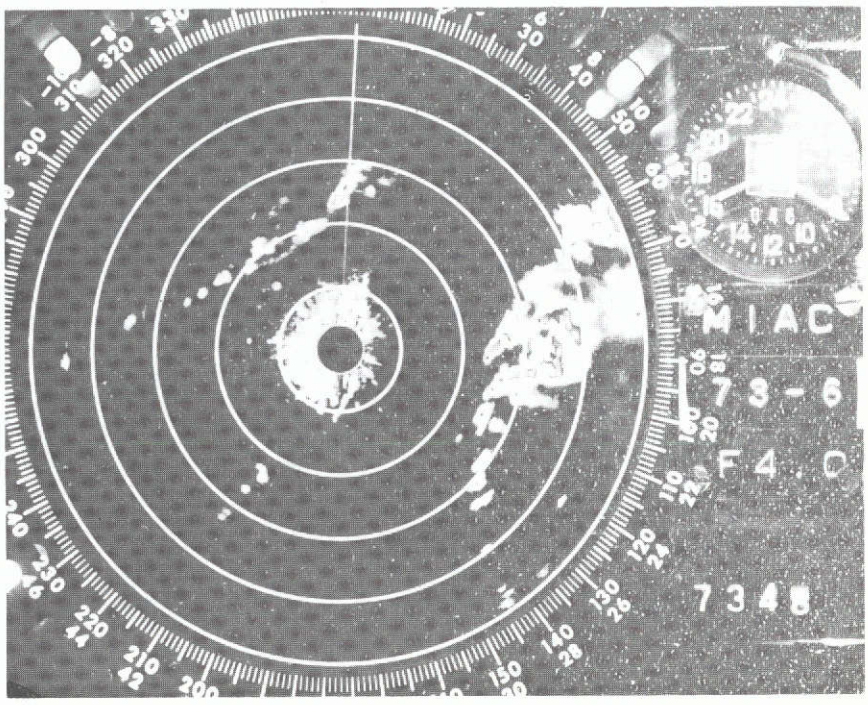

Figure 10b. National Weather Service WSR-57 (10 cm) Miami weather radar PPI polaroid image (VIP), recorded at 1620 GMT, February 15, 1973, 40-km (25-mile) range markers.

Figure 11 shows an example of a VIP radar image for 1620 GMT, February 15, 1973, superimposed upon the ESMR T_B analysis for 1623 GMT on February 15, 1973. It is seen that the location of warm T_B gradients detected by ESMR agree quite well with rain intensity gradients. However, the T_B values within the rain areas which included the high radiances emitted by land (Grand Bahamas Island) were not used in the statistics. In this analysis, 12 case studies were used, in which surface wind speeds in the area of the radar images were less than 7 meters per second and the atmosphere was considered to be subtropical maritime. Calculations by Nordberg, et al., 1971, showed that when sea surface winds were less than 7 meters per second, no changes in microwave brightness temperatures were noted. When sea surface winds were above 7 meters per second, a linear relationship between T_B and surface winds were noted if atmospheric conditions remained constant. For example, with sea

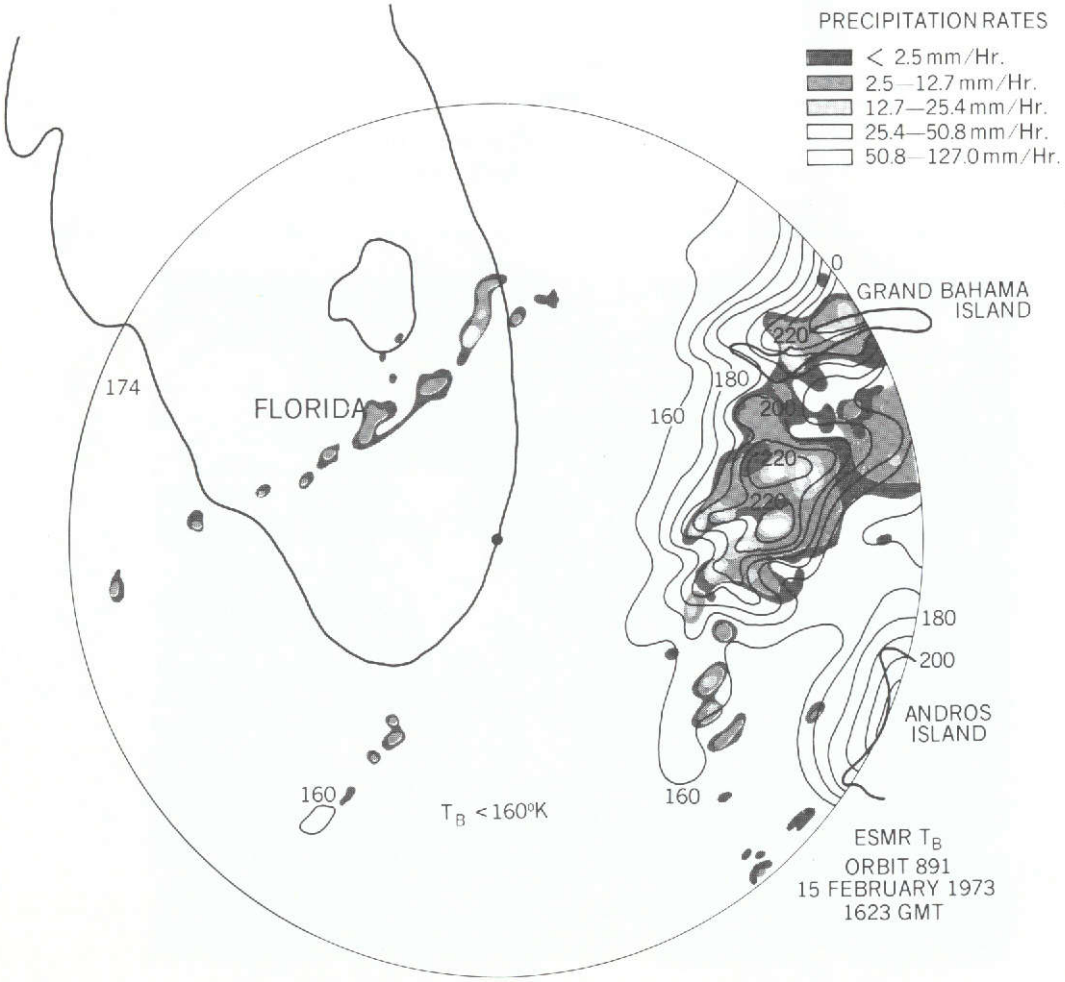

Figure 11. Hand-rectified National Weather Service WSR-57 (VIP) weather radar image from Miami for 1620 GMT, February 15, 1973, superimposed on a T_B analysis of individual scan spots from Nimbus-5 ESMR for 1623 GMT, February 15, 1973, orbit 891 (30° nadir angle limit).

surface winds of 20 meters per second, an additional increase of 15 K to the sea surface microwave brightness temperature was recorded by aircraft instruments.

The results of comparing ESMR data to WSR-57 data are shown in figure 12. The T_B values that fell within the four rain intensity categories are displayed at the mean of each category. For each category, the mean T_B and its standard deviation is shown by the solid and dashed lines respectively, and the mean T_B is listed in table 1.

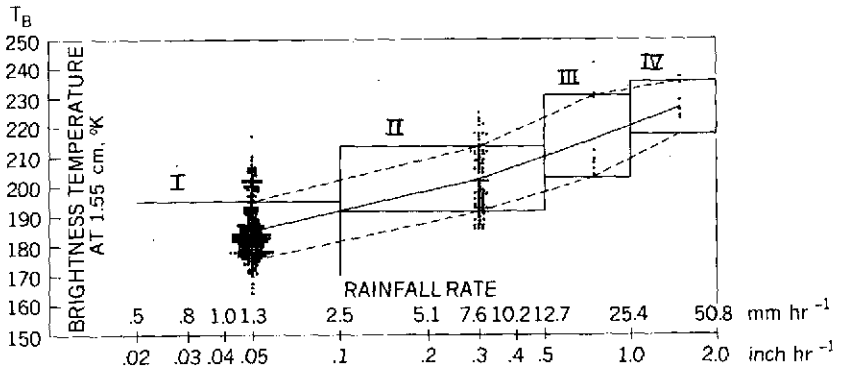

Figure 12. Four categories of Nimbus-5 ESMR brightness temperatures (°K) versus WSR-57 rainfall rates (VIP data) from Miami, Florida (December 1972 to February 1973).

Table 1
Comparison of Mean Rainfall Rate Data and
Mean ESMR T_B Data

Data	Category			
	I	II	III	IV
Mean Rainfall Rate (mm per hr)	1.3	7.6	19.0	38.1
Mean T_B (°K)	185 K	203 K	217 K	227 K
Standard Deviation	10 K	11 K	14 K	9 K

Because there were only nine cases of moderate to heavy rainfall rates in excess of 12.7 mm per hour, the results in Categories III and IV are statistically less significant.

In order to verify these empirical results, theoretical calculations of T_B versus rainfall rate were derived from a numerical model devised by Gaut and Reifenstein (private communication, 1973). The numerical model solves the equation of radiative transfer at points along the line of sight from a satellite looking toward the earth in the 19.35-GHz spectral region through a mean subtropical maritime atmosphere that contains precipitation at various rainfall rates. The model contains 30 layers, each 1-km thick, from the surface to 30 km, in which the temperature, pressure, density, water vapor, and molecular oxygen for the layer are determined from the mean of the parameter in each kilometer layer. The rain model contains one layer in which a uniform Marshall-Palmer droplet distribution is assumed for given rainfall rates from the surface to the freezing level at 4 km. The temperature of the liquid water droplets is 273 K and is isothermal throughout the layer. A calm ocean surface is used in the model, which assumes a smooth surface for which reflectivity can be calculated using the Fresnel equations for either horizontally or vertically polarized radiation.

The cross sections used in this calculation were the sum of the scattering and absorption coefficients, so that the rain effect is certainly overestimated at the higher rain rates. The results of the theoretical calculations are shown in the dashed curve in figure 13. The theoretical curve is almost linear up to 12 mm per hour and then becomes asymptotic to the 273 K. This indicates that for rainfall rates $>$ 18 mm per hour, the microwave energy detected by the Nimbus-5 ESMR will be emitted predominantly from the top of the rain column near the freezing level. The empirically derived data in figure 13 diverges from the theoretical calculations at the T_B value of 190 K. The reasons for the approximate 20 to 50 K negative difference are:

- The rain element detected by radar over the cold ocean background may not fill

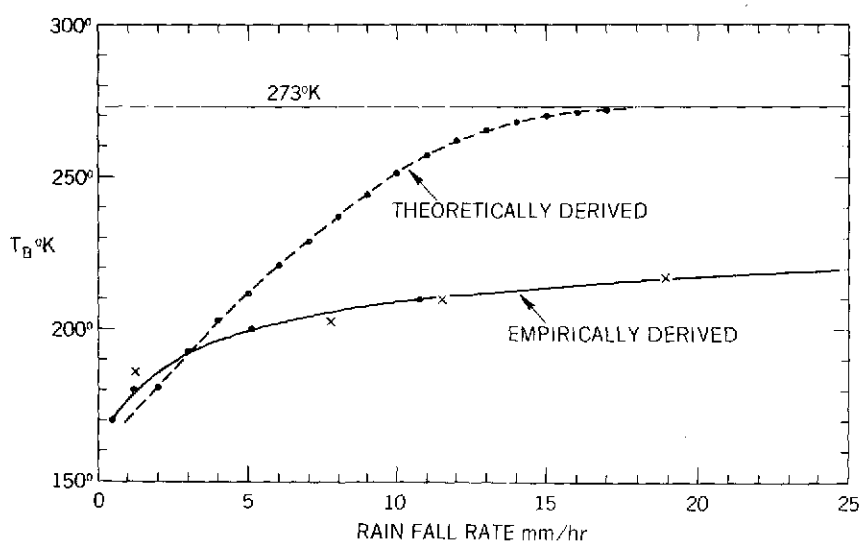

Figure 13. Nimbus-5 ESMR brightness temperatures (°K) versus rainfall rates (mm per hr), empirically derived (figure 12) and theoretically derived (Gaut Reifenstein, private communication, 1973).

the instantaneous field-of-view of the radiometer, especially in the heavier convective frontal showers and thunderstorms detected within 160 km (100 miles) of Miami.

- The approximation for the scattering effect used in the theoretical model.

For lighter, more continuous rainfall occurring over a larger area of stratiform clouds which fill the field-of-view of the radiometer, the ESMR rainfall rates and the theoretical calculations are in good agreement. Studies are now in progress (Rao and Theon, private communication, 1973) to attempt to estimate the latent heat of condensation released into the atmosphere by utilizing ESMR blackbody temperatures over oceanic rain areas. This term is extremely important in understanding the global heat budget, and is an essential input for numerical modeling of the atmosphere.

HYDROLOGICAL AND OTHER APPLICATIONS

The photofacsimile microwave images recorded by Nimbus-5 ESMR, almost from the first day of launch in December 1972, indicated a persistent soil moisture feature over the lower Mississippi Valley. Abnormally heavy precipitation occurred in October, November, and December, 1972, leaving the alluvial Mississippi Valley soils soaked with standing and subsurface water. Wet soils radiate as cold surfaces in the microwave imagery, which shows as white ground areas in figure 6a. A grid print map analysis was made for this area, shown in figure 14. Note that there are two major areas of T_B values < 220 K in the Mississippi Valley, which lie within a larger T_B, 240 K envelope. It was noted that this area overlaid the outwash aquifers in the drainage field, as shown in figure 15, which is from the National Atlas of the United States, 1970. A more complete study of the changes in these interesting hydrological features prior to the disastrous Mississippi River flood was made by Schmugge et al., 1974.

Another surface pattern verification of this feature is shown in the U.S. Air Force DAPP satellite IR imagery, which detected the same saturated soil area at 1205 GMT (0605 CST) on December 17, 1972 (figure 16). The same wet soil feature appeared warmer in the 8- to 13-μm channel. However, at approximately noon on January 22, 1973, the Nimbus-5 THIR (11-μm channel) showed no indication of this region (figure 17). This was probably due to solar heating which erased the nocturnal differences in surface temperatures that were present just after sunrise.

An analysis was made of the ESMR data (orbit 568), January 22, 1973, over the Gulf Stream in the north Atlantic, just south of Nova Scotia, under clear daytime sky conditions. Ship observations of sea surface temperature in this shipping lane varied from 8 to 19 K through the Gulf Stream. However, no indications of this sea surface temperature change were found in the ESMR data, which was approximately 140 K. Based upon the theoretical data from Lane and Saxton, 1952, the optimum microwave radiometric sensitivity to sea surface temperature was determined to be near the 5-cm wavelength (figure 18). This factor explains the insensitivity of ESMR to the Gulf Stream gradients described above.

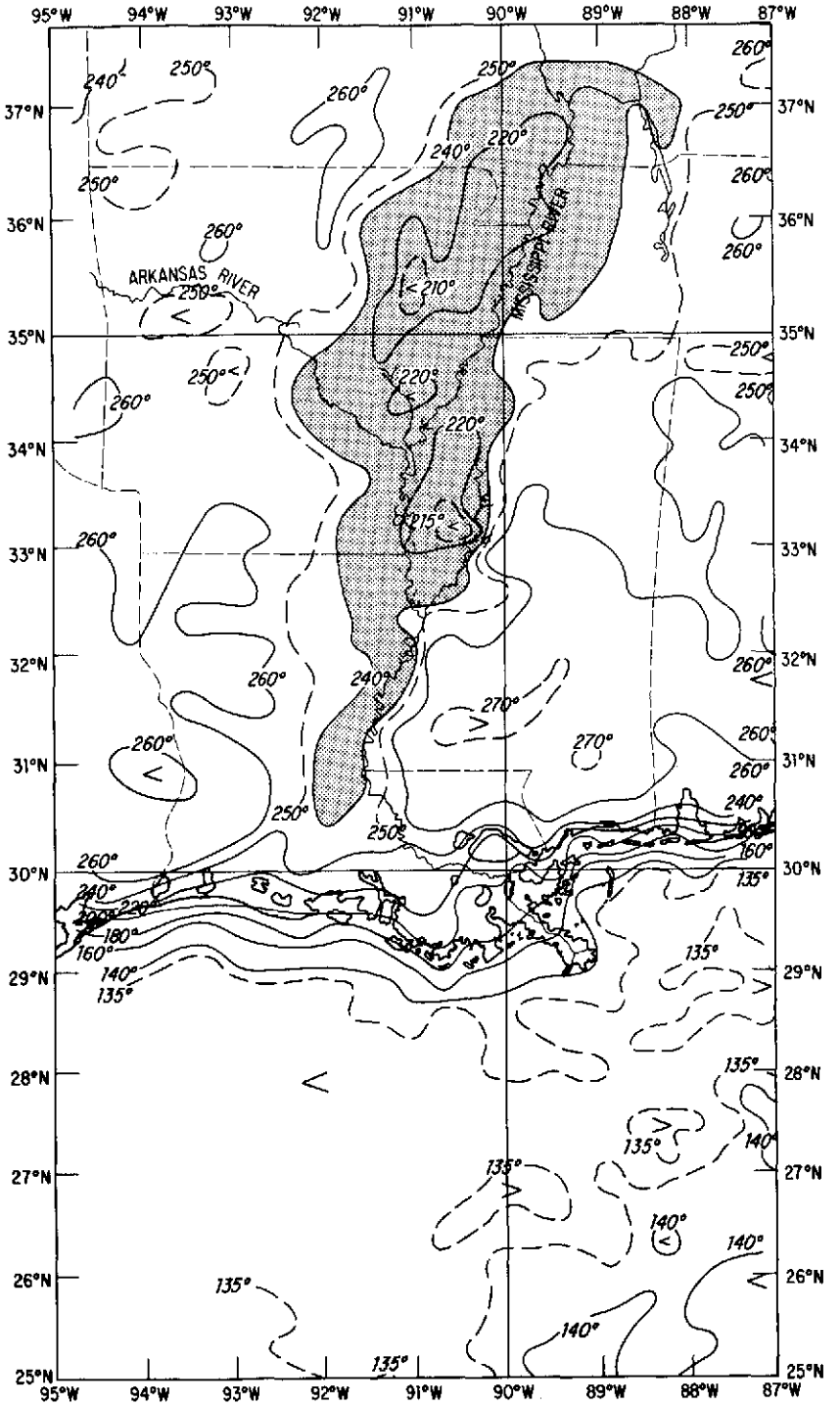

Figure 14. Nimbus-5 ESMR grid print map analysis, T_B in K, 1:2.5 million, Mercator, 1639 to 1643 GMT, daytime orbit 569, January 22, 1973, 19.35 GHz. (Dotted area: T_B <240 K.)

Figure 15. Map indicating region of outwash aquifers in the Mississippi Valley and approximate area of T_B <250 K in the Nimbus-5 ESMR data of figure 14.

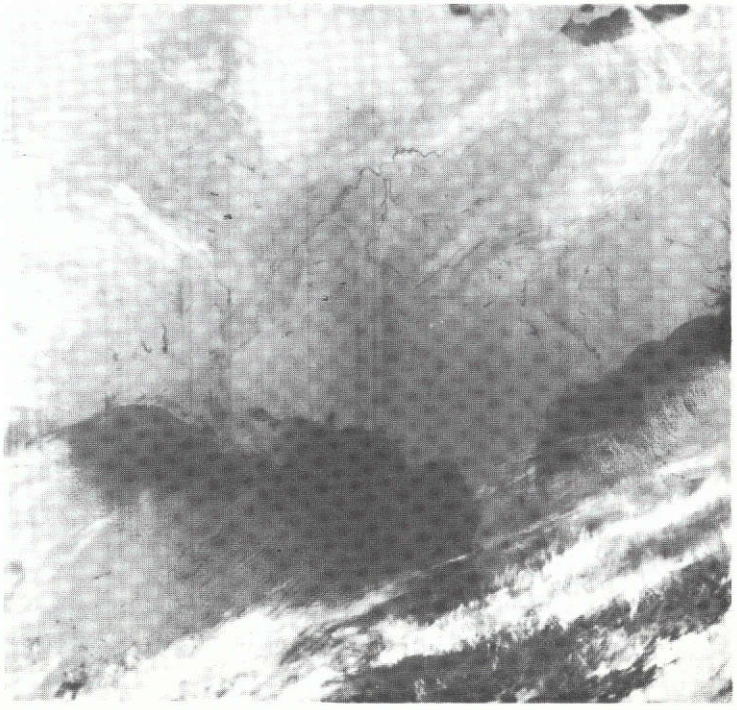

Figure 16. U.S. Air Force Data Acquisition and Processing Program (DAPP) image of IR data (8 to 13 μm), 1205 GMT, December 17, 1972, 617.3 m (1/3 n.m.) resolution.

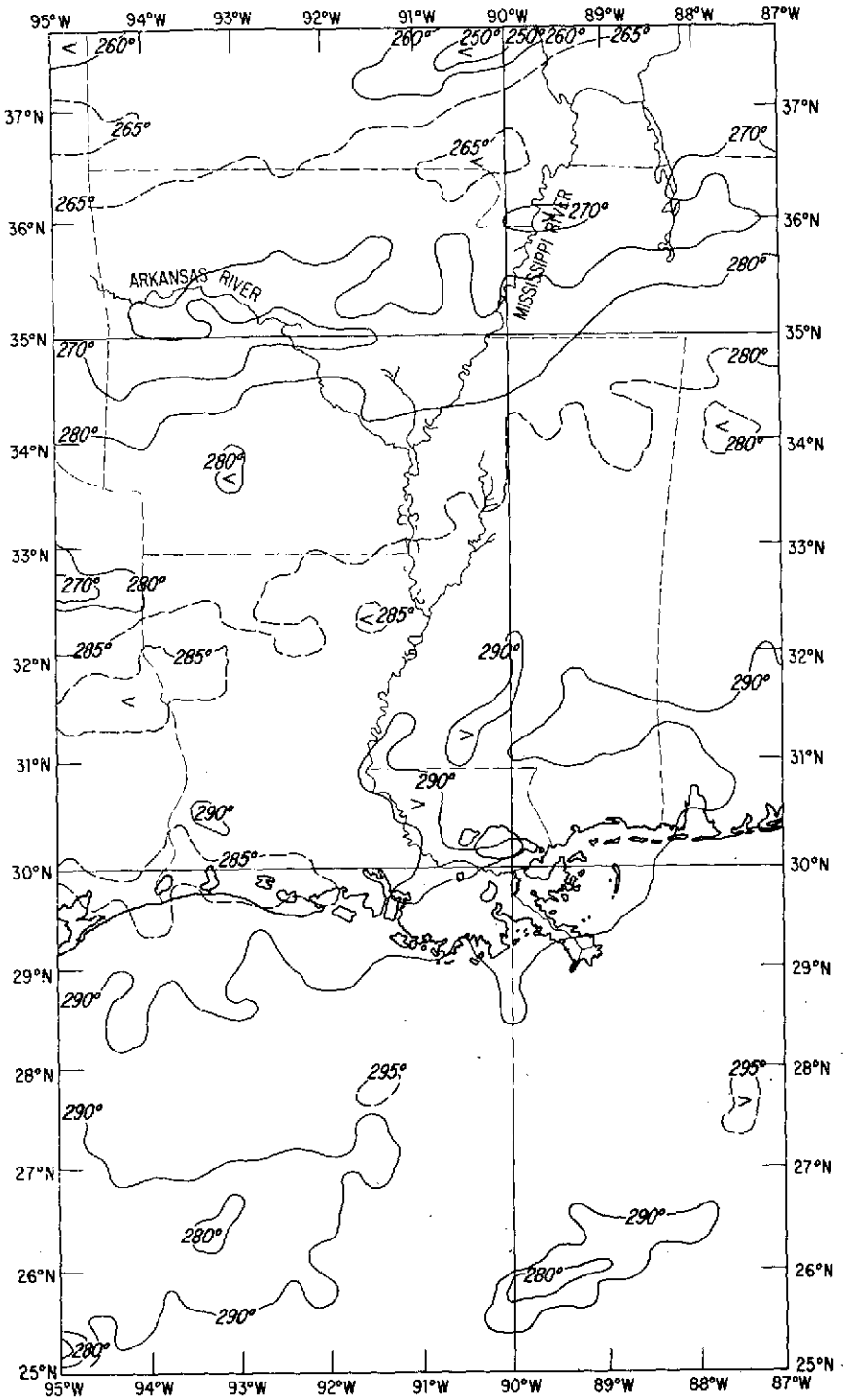

Figure 17. Nimbus-5 THIR grid print map analysis, T_B in °K, 1:2.5 million, Mercator 1639 to 1643 GMT, orbit 569 (day) January 22, 1973, 11 μm.

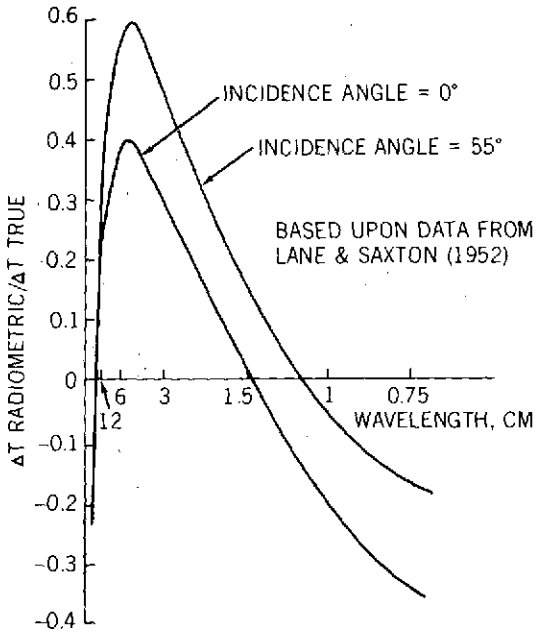

Figure 18. Radiometric temperature sensitivity for calm seawater, vertically polarized component (average sensitivity in the true range of 273 to 303 K (after Lane and Saxton, 1952).

Future polar orbiting satellites such as the Nimbus-F (1975) and -G (1978) will utilize different microwave frequencies which will be used to measure the meteorological, oceanographic, and hydrological parameters shown in figure 19.

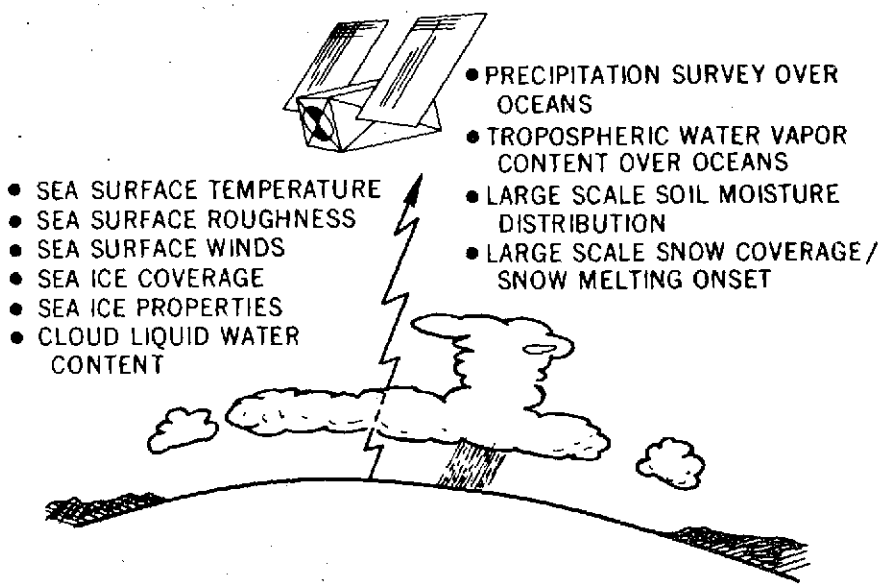

Figure 19. Future sensing objectives for multifrequency passive microwave radiometer system.

THE NIMBUS-5 TEMPERATURE-HUMIDITY INFRARED RADIOMETER (THIR) EXPERIMENT AND DATA ANALYSIS

The THIR flown on Nimbus-5 is a scanning bolometer which is similar to the one flown on Nimbus-4 (A. W. McCulloch, "The THIR Subsystem," *Nimbus 5 Users Guide,* NASA-GSFC, 1972). It contains two channels: a 10.5- to 12.7-μm window channel that provided night and day cloudtop or surface temperatures, with a ground resolution of 7.4 km (4 n.m.); and a 6.5- to 7.2-μm water vapor absorption channel, which peaks at 6.9 μm and senses the integrated moisture content of the upper atmosphere from 250 mbar (10.5 km) to 500 mbar (5.5 km), with a ground resolution of 24 km (13 n.m.) at the subsatellite point.

Figure 20 shows the photofacsimile imagery for orbit 569, January 22, 1973, for both the 6.7-μm THIR and ESMR data. The moisture-rich or cloudy regions are indicated by the white or light gray shading on the 6.7-μm imagery, while the drier areas are delineated by the

Figure 20. Nimbus-5 THIR (6.7 μm) and ESMR (19.35 GHz) photofacsimile images for 1633 to 1641 GMT, orbit 569 (day), January 22, 1973.

dark gray or black tones. The ESMR data show cloud droplets and/or rainfall over water as a warmer brightness temperature (darker gray to black) over a white (cold) background in this 190 K to 260 K range. Heavy clouds or rain occurring over land are shown better in the 250 to 290 K gray scale range.

The 6.7- and 11-μm photofacsimile film strips of orbit 570 shown in figure 21 show some striking differences and similarities. The east-west oriented cirrus clouds relating to the subtropical jet stream and scattered heavy cloud masses in the lower half of the pictures appear in both channels. However, the dark cyclonic streaks appearing in the upper half of the 6.7-μm strip do not appear in the 11-μm strip. Because the weighting function of the 6.7-

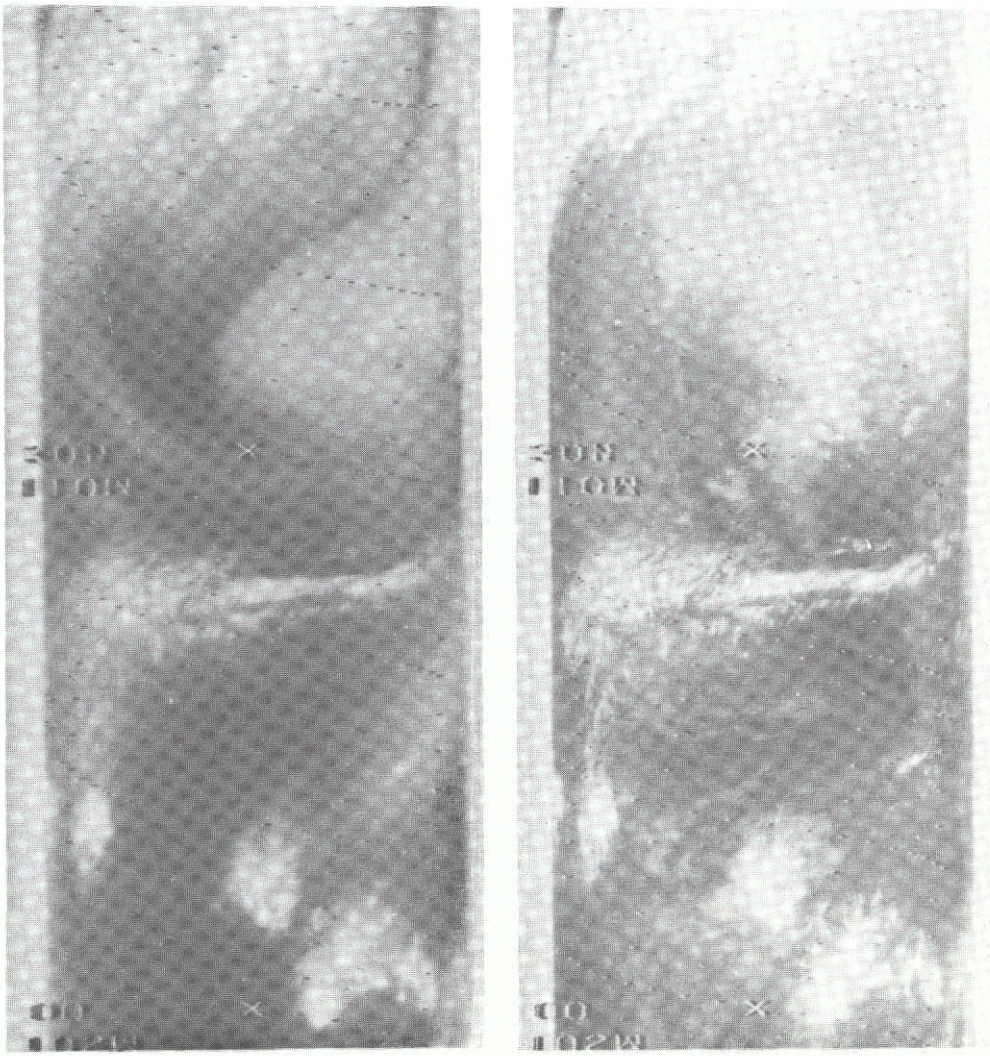

6.7 μm 11 μm

Figure 21. Nimbus-5 THIR (6.7 μm and 11 μm) photofacsimile images for orbit 570 (day), January 22, 1973.

μm channel peaks at 350 mbar, a 300 mbar chart at 00 GMT for January 23, 1973, was analyzed (figure 22). Note the strong ridge over the western U.S. and deep trough extending NE/SW from the Great Lakes to Arizona-New Mexico. Superimposed upon this constant pressure-height field is the location of the polar jet stream, 166 to 202 km hour (90 to 110 knots) descending on the west side of the trough, and the broad subtropical jet stream 202 to 230 km/hour (110 to 130 knots) ascending along the east side of the trough.

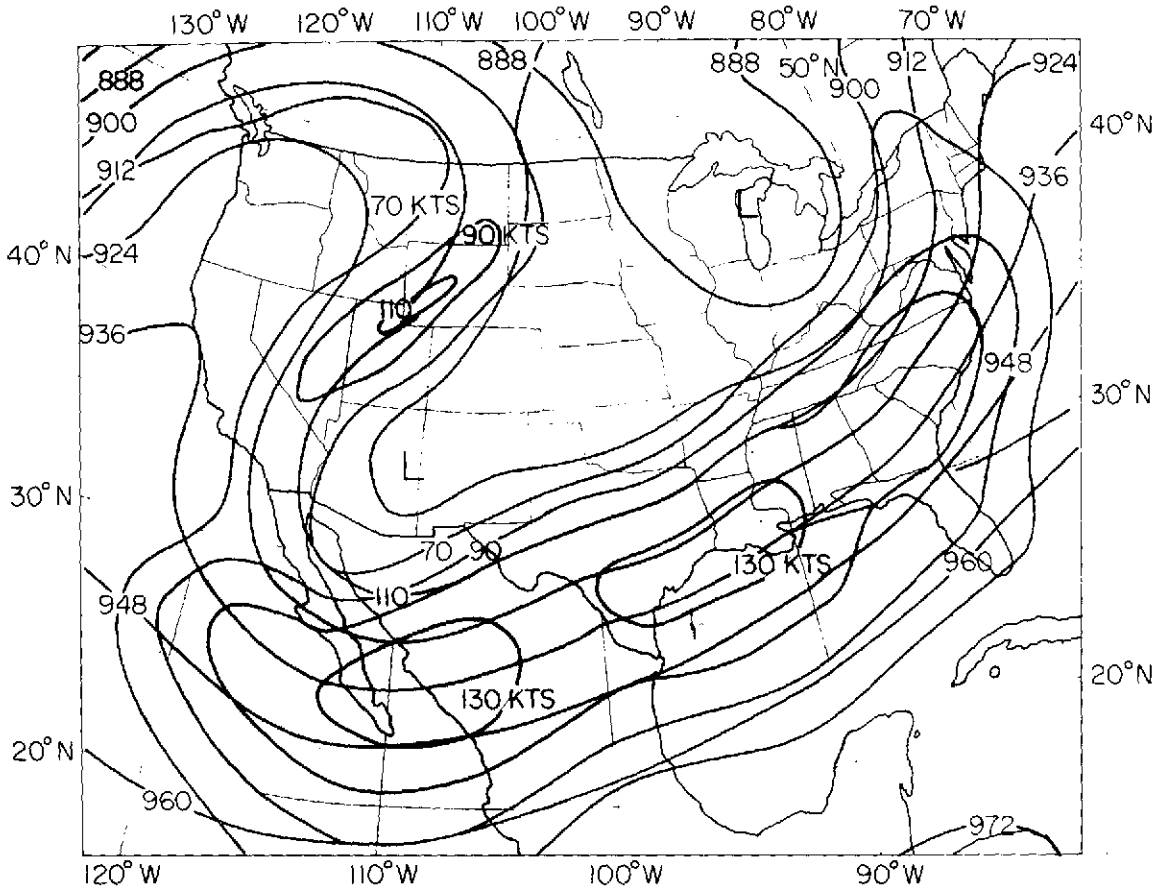

Figure 22. National Meteorological Center, National Weather Service 300-mbar chart, for 000 GMT, January 23, 1973. Jet streams on this chart are indicated by winds of over 70 knots (130 km/hr) at the 300-mbar level. (888 line = 9888 meters. Add 9,000 to numbers shown.)

Figure 23 shows the 1:2.5 million Mercator digital grid print map of the 6.7-μm data for orbit 569. The non-toned regions (brightness temperatures < 240 k) are areas of high clouds (light gray to white) and the cross-hatched-dotted areas are drier cloud-free zones ($T_B > 240$ K) (dark gray-black) in figure 21. Figure 24 shows the NMC 650 mbar level vertical velocity chart for 1200 GMT, January 22, 1973, which indicates broad areas of downward motion in the north side of the subtropical jet oriented NE/SW through Baja California and the Gulf states and along the eastern edge of the polar jet moving south-

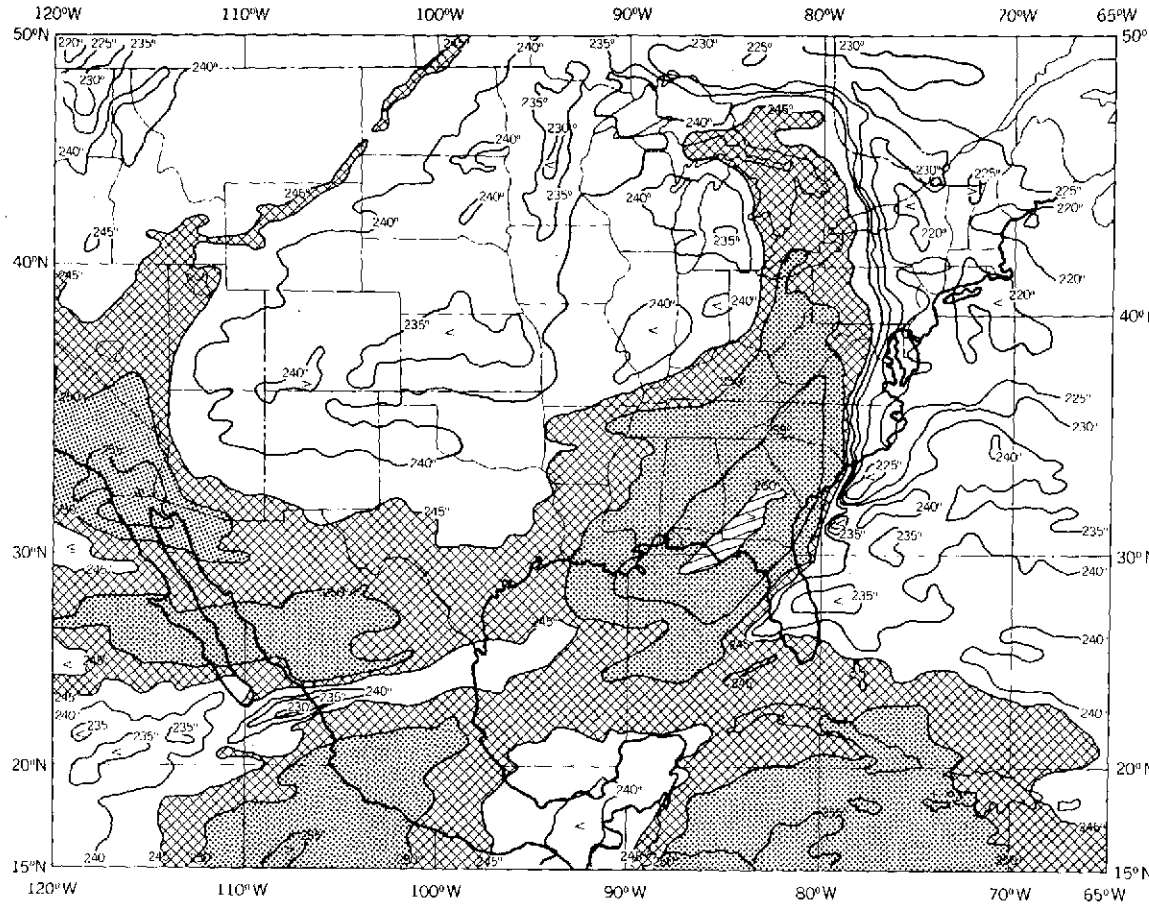

Figure 23. Nimbus-5 THIR (6.7 μm) grid print map analysis, T_B in K, 1:2.5 million, Mercator, 1637 to 1648 GMT, orbit 569 (day), January 22, 1973.

westward and descending over the Rocky Mountains. Previous studies by Martin and Salomonson (1970) over the U.S. have also related the warmer brightness values (darker areas along the northern edge of the subtropical jet) to areas of subsidence. Rodgers et al., (1973), have also described a synoptic situation in which areas of widespread and strong subsidence and advective areas of dry air correspond to areas delineated by high brightness temperatures in Nimbus-3, 6.7-μm MRIR data. An additional parameter that is apparent is that wind direction at the 300-mbar level (figure 22) is easily seen in the cyclonic pattern in this drier area of 6.7-μm data ($>$ 240 K) which outlines the edge of the two major jet streams (figure 23). Anticyclonic wind flow is also indicated southeast of Florida and Cuba in the 6.7-μm data which was confirmed in the 00 GMT NMC 300-mbar Northern Hemisphere charts for January 23, 1973. A qualitative comparison of the moisture patterns on the Nimbus-4 imagery with the 400-mbar level conventionally measured wind field had also indicated that the moisture patterns under near clear sky conditions aloft were generally aligned with the wind-field (Allison et al., 1972). The use of the 6.7-μm observations to improve midtropospheric wind flow analyses on a global scale has been discussed by Steranka

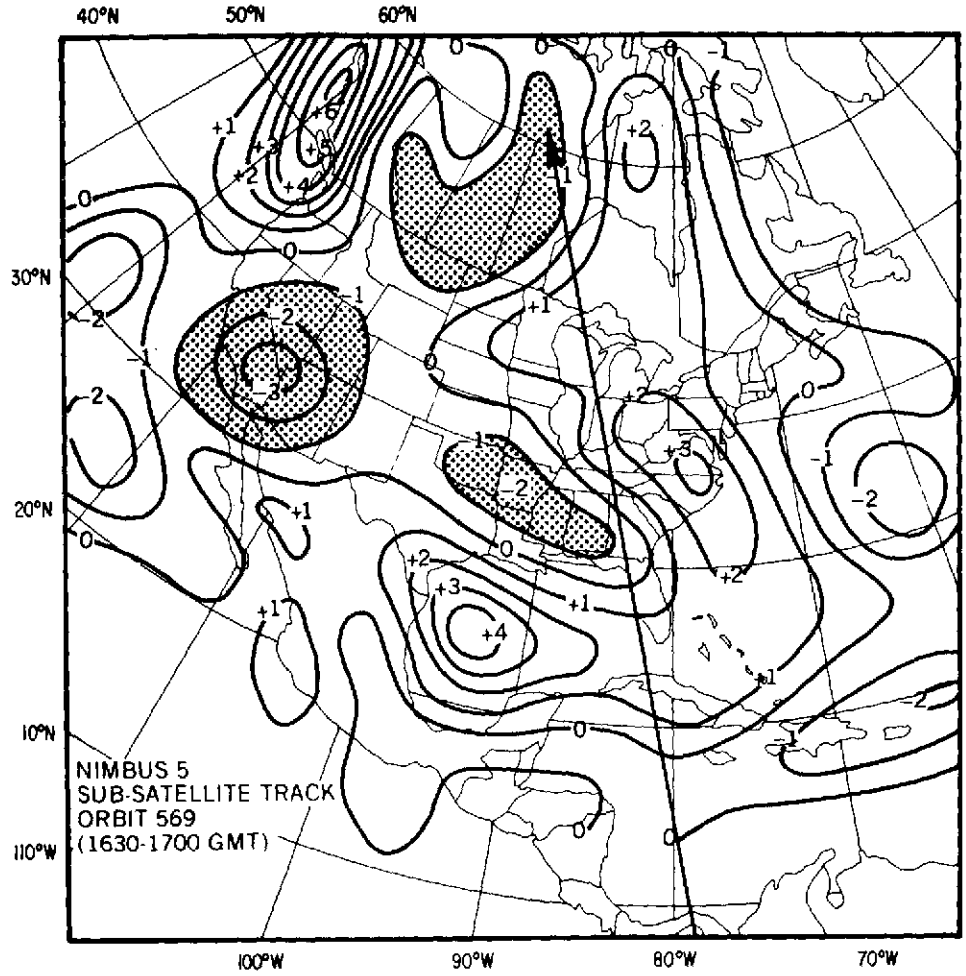

Figure 24. National Meteorological Center, National Weather Service, 650-mbar level vertical velocity chart (microbars sec^{-1}), 1200 GMT, January 22, 1973. (Dotted area: <1 mbar sec^{-1}.)

et al., 1973, and further research applying the Nimbus-5 THIR 6.7-μm data to the Goddard Institute for Space Studies Numerical Model is now in process.*

THE NIMBUS-5 VERTICAL TEMPERATURE SOUNDERS AND DATA ANALYSIS

The Nimbus-5 has three experiments which measure radiances needed to calculate the vertical temperature distribution of the atmosphere from the earth's surface to the stratosphere: the ITPR, the NEMS, and the SCR. The ITPR contains four channels in the 15-μm carbon dioxide band, one channel in the 19-μm rotational water vapor band, one in the 11-μm atmospheric window, and one in the 3.8-μm window. The instrument was designed to derive the temperature profile from the surface to 25 km with a vertical resolution of 3 to 5 km and an estimated accuracy of 2 K.

*R. Somerville, *The GISS Model of the Global Atmosphere*, NASA GSFC X-600-73-254, 1973.

The SCR has four optical filters and each filter contains four channels for a total of 16 channels whose range of measurement is from 2.06 μm to 133 μm. These channels permit the SCR to extend a temperature sounding up to 45 km with a 3- to 7-km vertical resolution and an estimated accuracy of 2 K.

The NEMS contains five channels, three tuned to the oxygen lines, near 60 GHz, one tuned to the 22-GHz water vapor line, and one tuned to the atmospheric window at 31 GHz. The NEMS provides a 192- by 192-km surface spatial resolution at nadir while the ITPR and SCR provide 35-km and 43-km instantaneous ground resolutions, respectively. The NEMS can sense atmospheric radiances even in the presence of clouds while the ITPR and SCR are strongly affected by clouds within their field-of-view (ERTS/Nimbus Project, *Nimbus-5 Users Guide*, NASA-GSFC, 1972; "GARP Project Data Systems Test Plan," NASA-GSFC, 1973). Figure 25 shows the weighting functions of each of the various channels of the

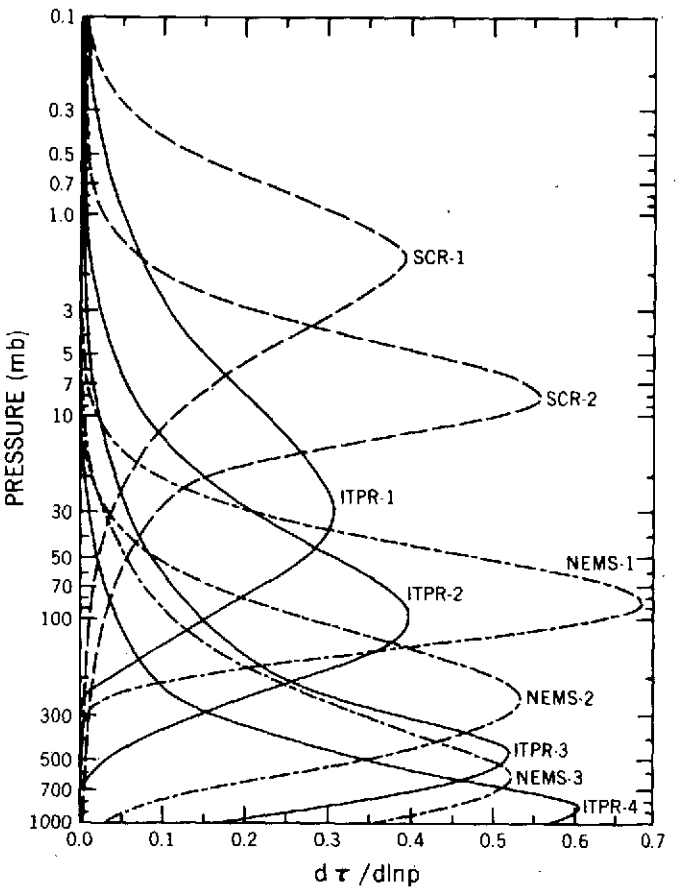

Figure 25. Atmospheric weighting function curves for Nimbus-5 ITPR, NEMS, and SCR spectral channels. Derivative of transmittance with respect to the logarithm of pressure (after Smith et al., 1973).

three vertical temperature sounding systems (Smith et al., 1973). Selected examples of the data amalgamation of these three systems during orbit 569, (1638 to 1651 GMT) for January 22, 1973, are shown in figure 26. (These sounding data were kindly provided by Drs. W. L. Smith and N. Grody, NESS, NOAA.) The 10 temperature profiles were taken in regions of variable relative humidity and cloudiness along the Nimbus-5 subsatellite track from the subtropics to the Arctic Circle (figure 27). Radiosonde data (1200 GMT) from stations near to the satellite track were plotted for comparison.

Table 2 shows the differences between the conventional and satellite-derived temperature by constant pressure level. Note that there are four levels with the following mean temperature differences: 850 mbar, +2.4 K; 700 to 250 mbar, -1.8 K; 200 to 100 mbar, +1.3 K; and 70 to 20 mbar, -2.4 K.

A positive value indicates that the radiosonde air temperatures are warmer than the satellite-derived vertical air temperature. The mean of the layer mean differences from 850 to 20 mbar was -0.9 K.

A comparison (table 3) was made of the 1000 to 500 mbar level thickness which was derived from the NEMS and NMC thickness data along the Nimbus 5 subsatellite track of orbit 569

Table 2
Difference (in °K) Between Related 1200 GMT Radiosonde Ascents and Nimbus-5 Vertical Soundings Recorded During Orbit 569 on January 22, 1973, from 23.3°N to 72.7°N

	23.3°N	26.8°N	30.3°N	33.7°N	37.9°N	41.9°N	47.3°N	54.8°N	58.6°N	72.7°N	Mean
1000 mbar	+6.0°	–	–	–	–	–	–	–	–	–	–
850 mbar	+4.5°	-1.3°	+3.7°	+1.1°	+1.6°	+4.7°	+5.9°	+3.6°	+5.7°	-5.8°	+2.4°
700 mbar	-4.4°	-6.1°	-3.4°	-0.6°	+5.9°	+2.0°	+1.0°	-3.6°	+5.7°	-1.1°	-0.5°
500 mbar	-2.6°	-4.7°	-5.0°	-3.7°	+0.4°	-5.6°	-1.1°	-6.3°	+2.0°	-0.2°	-2.7°
400 mbar	-4.8°	-7.3°	-2.9°	-6.7°	-3.0°	-0.8°	-1.4°	-4.8°	+2.6°	+1.1°	-2.8°
300 mbar	-2.9°	-4.7°	-5.2°	-1.3°	-1.4°	+2.4°	-2.9°	-2.7°	-4.2°	+2.4°	-2.1°
250 mbar	-1.3°	-0.1°	-3.3°	+5.7°	+0.7°	-1.0°	-3.6°	-2.2°	-7.4°	-0.2°	-1.3°
200 mbar	+2.4°	+2.6°	+4.3°	+6.2°	+0.3°	-1.5°	-1.7°	+3.0°	-2.9°	-2.6°	+0.8°
150 mbar	+5.3°	+4.6°	+6.1°	+2.8°	+2.1°	+2.1°	+3.2°	+5.5°	+0.1°	-1.8°	+3.0°
100 mbar	+2.9°	+1.5°	+0.1°	-2.7°	-4.3°	+2.6°	+0.6°	+1.9°	-1.1°	+0.9°	+0.2°
70 mbar	-2.5°	-3.3°	+1.1°	-0.6°	-3.8°	-1.9°	-3.0°	-0.4°	-3.6°	+1.5°	-1.7°
50 mbar	-3.8°	+0.2°	–	-1.2°	-1.0°	-1.3°	–	-3.3°	-7.2°	+0.7°	-2.1°
30 mbar	-1.5°	-0.9°	–	-1.8°	-3.4°	-3.1°	–	-5.3°	-4.2°	-5.7°	-3.1°
20 mbar	+2.7°	+0.5°	–	+0.7°	-4.2°	-1.8°	–	–	-9.5°	–	-1.9°
Sources of Data	ITPR, NEMS, SCR			NEMS, SCR (OVERCAST SKIES)				ITPR, NEMS, SCR			-0.9° Overall Mean

* Plus sign (+) indicates the radiosonde data is warmer than the satellite data, - indicates the radiosonde data is colder than the satellite data.

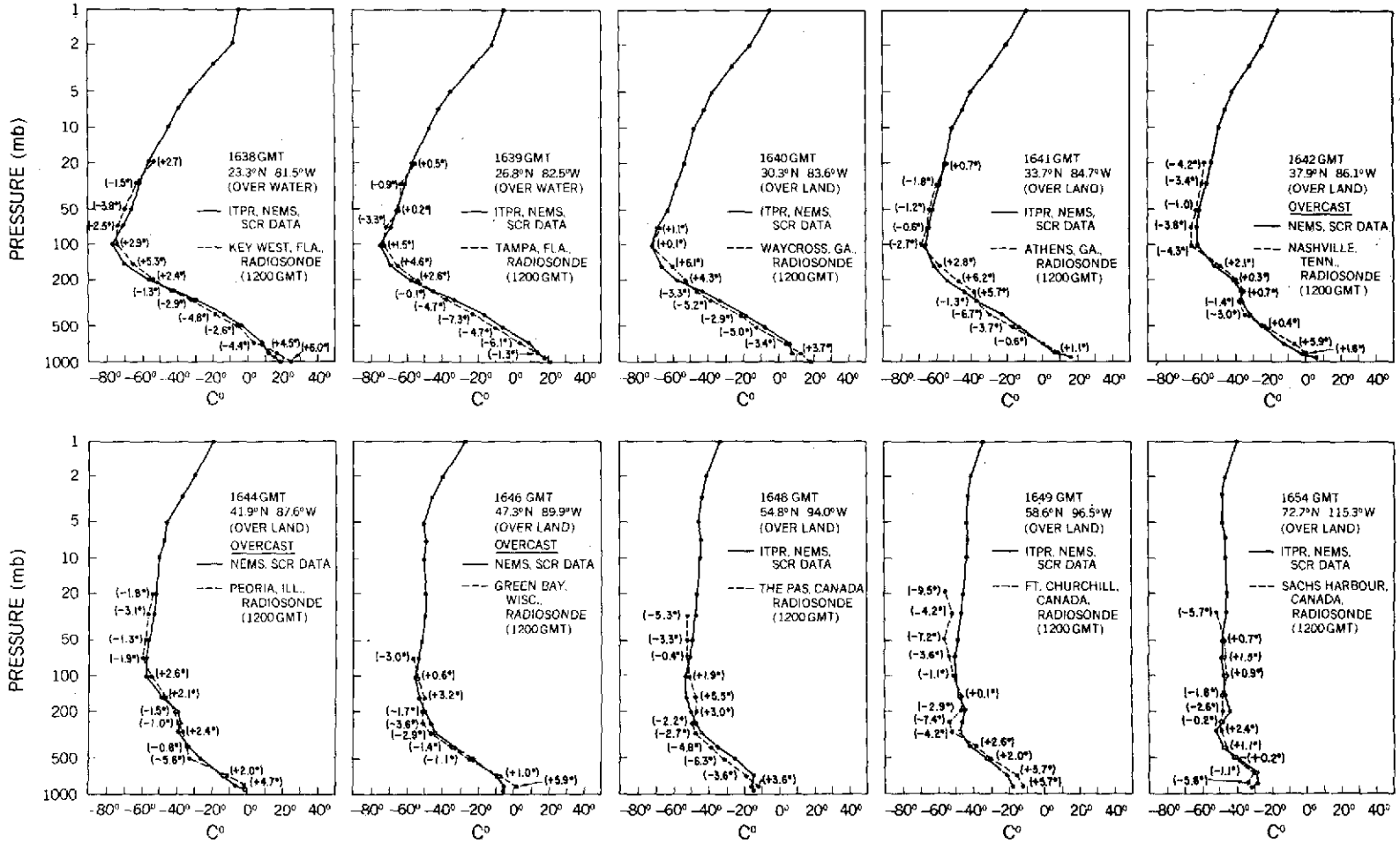

Figure 26. Nimbus-5 vertical temperature soundings derived from ITPR, NEMS, and SCR radiances, 1638 GMT to 1654 GMT, orbit 569, January 22, 1973, and related 1200 GMT radiosonde data. (A positive value indicates that the radiosonde air temperature is warmer than the satellite-derived air temperature.)

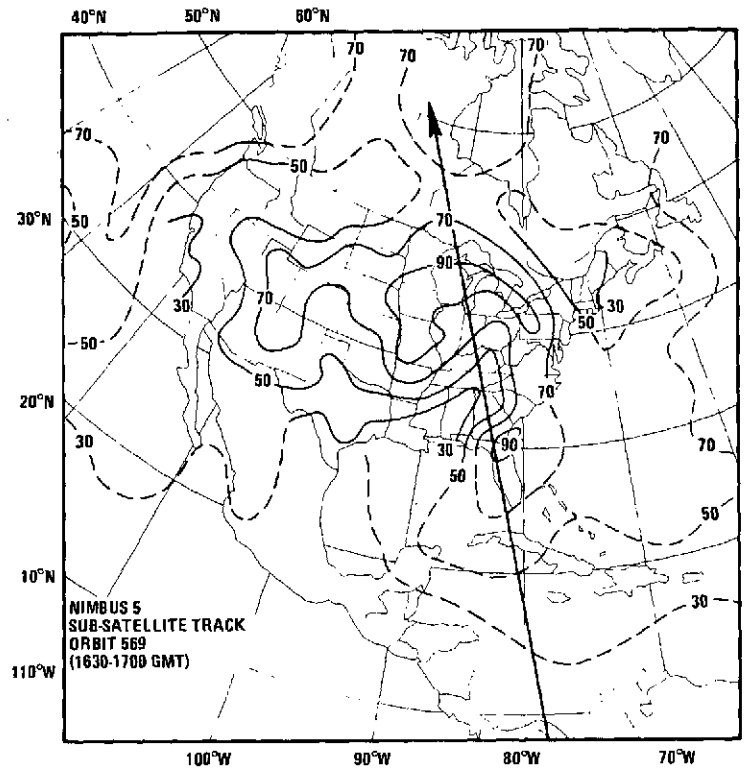

Figure 27. National Meteorological Center, National Weather Service, average relative humidity chart (%), surface to 500-mbar, 1200 GMT, January 22, 1973.

(figure 28). (The NEMS and NMC data were kindly provided by Prof. D. H. Staelin and R. L. Pettyjohn of MIT.) The change in sign and magnitude of the thickness difference at 23.43°N, 30.47°N, and 61.55°N were due to a change in the algorithm used in the basic computer program used to derive these thicknesses. The negative sign indicates that the NEMS derived thickness is less than the NMC measured thickness. The largest differences appear to be between approximately 40° to 60°N.

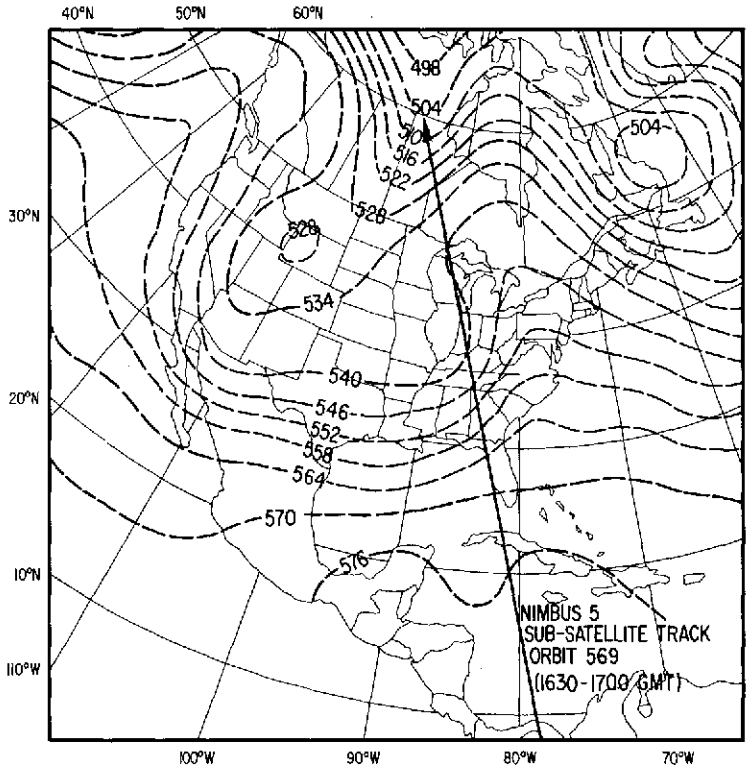

Figure 28. National Meteorological Center, National Weather Service 1000- to 500-mbar thickness chart (meters), 1200 GMT, January 22, 1973.

Table 3
Comparison of Level Thickness

Latitude	Difference (meters)	Latitude	Difference (meters)	Latitude	Difference (meters)
19.02°N	-7	35.74°N	-40	52.23°N	-69
19.90°N	-2	36.61°N	-48	53.09°N	-70
20.78°N	-4	37.49°N	-51	53.95°N	-78
21.66°N	-4	38.36°N	-48	54.80°N	-63
22.55°N	0	39.23°N	-53	55.65°N	-62
23.43°N	+7	40.11°N	-72	56.50°N	-74
24.31°N	+12	40.98°N	-51	57.35°N	-59
25.19°N	+16	41.85°N	-73	58.19°N	-54
26.07°N	+19	42.72°N	-77	60.71°N	-5
26.95°N	+28	43.59°N	-76	61.55°N	+2
27.83°N	+39	44.46°N	-87	62.38°N	+10
28.71°N	+55	47.06°N	-74	63.20°N	+27
29.59°N	+72	47.93°N	-71	64.03°N	+36
30.47°N	-5	48.79°N	-82	64.85°N	+32
33.11°N	-22	49.65°N	-75	65.66°N	+31
33.98°N	-28	50.51°N	-80	66.47°N	+36
34.86°N	-29	51.37°N	-74	67.27°N	+49

CONCLUSION

It has been shown that the Nimbus-5 ESMR and THIR can be used together as a multispectral analysis tool. The thermal microwave emission at 1.55 cm as recorded by the ESMR is sufficiently different from the IR and visible region due to radiative transfer characteristics to provide unique and practical applications for meteorology, oceanography, and hydrology.

The utilization of the ITPR, NEMS, and SCR data to produce an amalgamated sounding, can produce significantly better profiles than can be achieved individually (Smith et al., 1973). The incorporation of these data to be returned from the improved Nimbus-F vertical sounders (1975) into the new high resolution numerical models at the National Meteorological Center and the Goddard Institute for Space Studies is expected to make a positive impact on the 12 to 24 hour forecast problem.

ACKNOWLEDGMENTS

The authors wish to acknowledge the assistance of Lt. Colonel H. Brandli, Det. 11, 6th Weather Wing, Patrick AFB, Florida, in obtaining FPS-77 weather radar data; Dr. W. L. Woodley, and C. G. Griffith, Experiments Meteorology Laboratory, NOAA, Coral Gables, Florida, in obtaining WSR-57 radar data; Mr. Mark Smith for his work in analyzing the WSR-57 radar data; Mr. John Theon, GSFC; and Major Lee Dickenson, Hqtrs., Air Weather Service, USAF, for the use of several figures in this paper.

Goddard Space Flight Center
National Aeronautics and Space Administration
Greenbelt, Maryland August 1974
910-175-61-41-01

REFERENCES

Aerojet Electrosystems Co., *Meteorological Applications of Passive Microwave Radiometry*, Final Report, SAMSO TR No. 73-206, Vol. III, Part I and II, 1750 FR-1, Azuaz, California, 1973.

Allison, L. J., J. Steranka, G. T. Cherrix, E. Hilsenrath, "Meteorological Applications of the Nimbus 4 Temperature-Humidity Infrared Radiometer, 6.7 μm Channel Data," *Bull. of the American Meteorological Society*, **53**, No. 6, 1972, pp. 526-535.

Battan, L., *Radar Meteorology*, University of Chicago Press, Chicago, Illinois, 1959.

Campbell, W. J., P. Gloersen, W. Nordberg, T. T. Wilheit, "Dynamics and Morphology of Beaufort Sea Ice Determined from Satellites, Aircraft and Drifting Stations;" Paper A.5.6, (to be published: *The Proceedings of Symposium on Approaches to Earth Sciences Through the Use of Space Technology*), Cospar, Working Group 6, Constance, Germany, 1973.

Catoe, C., W. Nordberg, P. Thaddeus, G. Ling, *Preliminary Results from Aircraft Flight Tests of an Electrically Scanning Microwave Radiometer*, NASA TM X-55893, 1967.

ERTS/Nimbus Project, *The Nimbus 5 Users Guide*, NASA, Goddard Space Flight Center, Greenbelt, Maryland, 1972.

Follansbee, W., *Estimation of Average Daily Rainfall from Satellite Cloud Photographs*, NOAA Tech. Memo. NESS 44, National Environmental Satellite Service, NOAA, Washington, D. C., 1973, 39 pp.

Gloersen, P., W. Nordberg, T. J. Schmugge, T. T. Wilheit, W. J. Campbell, *Microwave Signatures of First-Year and Multi-Year Sea Ice*, NASA TM X-66006, 1972.

Gloersen, P., T. C. Chang, T. T. Wilheit, W. J. Campbell, *Polar Sea Ice Observations by Means of Microwave Radiometry*, NASA TM X-70529, 1973a.

Gloersen, P., W. Nordberg, T. J. Schmugge, T. T. Wilheit, "Microwave Signatures of First Year and Multi-Year Sea Ice," *J. Geophys. Res.*, 78, 1973b, 3564-3572.

Gloersen, P., T. T. Wilheit, T. C. Chang, W. Nordberg and W. J. Campbell, *Microwave Maps of the Polar Ice of the North*, NASA TM X-70493, 1973c.

Gunn, K. L. S. and T. U. R. East, "The Microwave Properties of Precipitation Particles," *Quart. J. Met. Soc.*, **80**, 1954, 522-545.

Hollinger, J. P., "Passive Microwave Measurements of Sea Surface Roughness," *IEEE, Trans. on Geoscience Electronics*, GE-9, No. 3, 1971, 165-169.

Lane, J. A. and J. A. Saxton, "Dielectric Dispersion in Pure Polar Liquids at Very High Radio-Frequencies," *Proc. Roy. Soc.* A214: 1952, 400-545.

Leighton, R. B., *Principles of Modern Physics*, McGraw-Hill Book Co., New York, New York, 1959.

Martin, F. L. and V. V. Salomonson, "Statistical Characteristics of Subtropical Jet Stream in Terms of MRIR Observations from Nimbus 2," *J. of Applied Met.*, **9**, No. 3, 1970, p. 508-520.

Martin, D. W. and W. D. Scherer, "Review of Satellite Rainfall Estimation Methods," *Bulletin of the American Meteorological Society*, **54**, No. 7, 1973, p. 661-674.

National Atlas of the United States of America, United States Department of the Interior, Geological Survey, Washington, D. C., 1970.

Nordberg, W., J. Conaway and P. Thaddeus: "Microwave Observations of Sea State from Aircraft," *Quart. J. Roy. Meteorological Society*, **95**, 1969, p. 408.

Nordberg, W., J. W. Conaway, D. B. Ross and T. Wilheit, "Measurement of Microwave Emission from a Foam-Covered Wind Driven Sea," *J. Atmos. Sci.*, 28, No. 3, 1971, 429-435.

Paris, J. F., *Microwave Radiometry and Its Application to Marine Meteorology and Oceanography*, Ref. No. 69-IT, Dept. of Oceanography, Texas A&M University, College Station, Texas, 1969.

Paris, J. F., *Transfer of Thermal Microwaves in the Atmosphere*, II, Dept. of Meteorology, Texas A&M University, College Station, Texas, Contract Final Report, NASA Grant NGR 44-001-098, NASA, GSFC, 1971, 211 pp.

Porter, R. A. and F. J. Wentz, III: *Research to Develop a Microwave Radiometric Ocean Temperature Sensing Technique*, Final Report, Vol. 1, 2, Radiometric Technology Inc. Wakefield, Mass., 1972, Contract 2-35309, for USDOC, NOAA, NESS.

Rodgers, E. B., V. V. Salomonson, and H. L. Kyle, *Upper Tropospheric Dynamics as Reflected in the Nimbus 4 THIR 6.7 μm Data*, NASA TN D-7493, 1973, pp. 27.

Ross, D. B., V. T. Cardone, and J. W. Conaway, "Laser and Microwave Observations of Sea Surface Condition for Fetch-Limited 17 to 25 m/sec Winds," *IEEE Trans. on Geoscience Electronics*, GE-8, No. 4, 1970, p. 326-336.

Sabatini, R. R. and E. S. Merritt, *The Nimbus 5 ESMR and Its Application to Storm Detection*, Final Report Contract No. N62306-72-C-0153, Environmental Prediction Research Facility, U.S. Navy, Monterey, California, 1973.

Schmugge, T., P. Gloersen and T. T. Wilheit, *Remote Sensing of Soil Moisture with Microwave Radiometers*, NASA TM X-66265, 1972.

Schmugge, T., A. Rango, L. J. Allison, and T. T. Wilheit, *Hydrologic Applications of Nimbus 5 ESMR Data*, NASA TM X-66201, 1974, pp. 21.

Skidmore, R. W. and J. F. W. Purdom, *Application of Meteorological Satellite Data in Analysis and Forecasting*, Supplement #2 to ESSA Tech. Report NESC 51, U.S. Department of Commerce, NOAA, NESS, Washington, D. C., 1973, 59 pp.

Smith, W. L., D. H. Staelin and J. T. Houghton, "Vertical Temperature Profiles from Satellites - Results from Second Generation Instruments Aboard Nimbus 5," presented at the COSPAR Symposium on Approaches to Earth Survey Problems Through the Use of Space Techniques, Konstanz, F. R. of Germany, May 23-June 6, 1973.

Steranka, J., L. J. Allison and V. V. Salomonson, "Application of Nimbus 4 THIR 6.7 μm Observations to Regional and Global Moisture and Wind Field Analyses," *Journal of Applied Meteorology*, Vol. 12, No. 2, 1973, pp. 386-395.

Theon, J., "A Multispectral View of the Gulf of Mexico from Nimbus 5," *Bulletin of the American Meteorological Society*, Vol. 54, No. 9, 1973, pp. 934-937.

U.S. Department of Commerce, *Satellite Data Requirements of Atlantic Oceanographic and Meteorological Laboratories for Studies of Ocean Physics and Solid Earth*, NOAA Technical Report ERL 225-AOML 5, Environmental Research Laboratories, Boulder, Colorado, 1971, 46 pp.

Wilheit, T. T., J. C. Blinn, W. Campbell, A. Edgerton and W. Nordberg, 1972: "Aircraft Measurements of Microwave Emission from Arctic Sea Ice," *Remote Sensing of the Environment*, 2, 1972, pp. 129-139.

Wilheit, T. T., J. Theon, W. Shenk, and L. J. Allison, *Meteorological Interpretations of the Images from Nimbus 5 Electrically Scanned Microwave Radiometer*, NASA TM X-70424, 1973, pp. 21.